IS-T-924

High-Temperature Chlorination Of Coal Fly Ash

MASTER

by

Douglas John Adelman

M.S. Thesis submitted to Iowa State University

Ames Laboratory, DOE
Iowa State University
Ames, Iowa 50011

Date Transmitted:

PREPARED FOR THE U.S. DEPARTMENT OF ENERGY
UNDER CONTRACT NO. W-7405-eng-82

DISCLAIMER

Printed in the United States of America

Available from
National Technical Information Service
U.S. Department of Commerce
5265 Port Royal Road
Springfield, VA 22161

High-temperature chlorination of coal fly ash

by

Douglas John Adelman

A Thesis Submitted to the
Graduate Faculty in Partial Fulfillment of the
Requirements for the Degree of
MASTER OF SCIENCE

Major: Chemical Engineering

Approved:

Geo. Burnet
In Charge of Major Work

M A Larson
For the Major Department

M J Ulmer
For the Graduate College

Iowa State University
Ames, Iowa

1980

TABLE OF CONTENTS

LIST OF TABLES

LIST OF FIGURES

INTRODUCTION

Coal has been and will continue to be a major energy source. When pulverized coal is combusted, an inorganic, unburnt portion, fly ash, remains. Many previous sources (5a, 10, 51, 52) have described the fly ash production rates and its possible uses. Fly ash is being considered here as a source of aluminum and possibly titanium. The HiChlor process (9) has been proposed and outlines the steps necessary to extract and purify the metals from fly ash. A reduction-chlorination reaction is suggested as the step to remove the metals from fly ash. The fly ash is exposed at elevated temperatures to a reductant and chlorine, and volatile metal chlorides are produced. The purpose of the work reported here was to study this gas-solid reaction.

Test conditions were specified, experiments conducted, and the results analyzed in an effort to decide what limited the reaction rates and the final fly ash conversions. With such information, operating conditions can be specified and equipment designed to improve the yields and efficiency of the reaction.

Gas-solid reaction limitations fall into two categories: chemical or physical. Chemical control generally results from kinetic effects. The free energy changes are large and negative for the reduction-chlorination reactions involved, therefore, equilibrium thermodynamics probably will not control the reaction rates. Physical factors include mass transfer and the surface area of the solid. Mass transfer limitations can result from slow diffusion through a stagnant film surrounding the particles or from slow diffusion in and out of particle pores. The reaction rate is truly proportional to the surface area only if kinetics or thermodynamics limit the reaction. If mass transfer limits, then the surface area is not fully utilized.

A great deal of information is needed before final decisions can be made concerning reaction limitations or mechanisms. As a first step, it was necessary to determine the chemical nature of fly ash. Elemental compositions were determined but also, the actual compound constituents of fly ash were found to be important. Fly ash contains four major elements, iron, aluminum, silicon, and calcium. The iron generally appears as magnetite, the aluminum and silicon are combined into a glass, and the calcium appears mostly as calcium oxide on the ash particle surfaces (8). There is some iron spread throughout the silica-alumina glass and a small amount of the silica appears as quartz. It is important to know the compound constituents if thermodynamic calculations are to be useful and if reaction mechanisms are to be proposed.

Such information as particle size distributions and specific surface areas were obtained over a range of fly ash conversions. These data are needed for determining whether mass transfer or specific surface area is limiting the reaction.

Fly ash chlorinations were next conducted using graphite as the reductant. The fly ash was magnetically separated to give an iron rich and an iron poor fraction. The iron poor or nonmagnetic fraction was used in all chlorinations. The fly ash to graphite weight ratio was always 10:3, the sample size was 10 grams, and the chlorine flow was 0.0010 g-moles/min for one set of experiments and 0.0013 g-moles/min for a second set. The reaction temperatures used were 750, 800, 850 and

900°C, the reaction periods were 1/2, 1, and 2 hours, and the total pressure was about 1 atmosphere. All chlorinations were done in a horizontal, fixed-bed reactor.

Some nonmagnetic fly ash was leached with dilute hydrochloric acid to remove the calcium oxide. Then, in the first series of experiments, leached and nonleached nonmagnetic fly ash samples were chlorinated to test the effects of leaching. In a second set of experiments, only leached nonmagnetic fly ash was chlorinated at the same temperatures but, for only 2-hour periods with continuous chromatographic analyses of the noncondensible fraction of the product gas stream. In all of the chlorination experiments, the amounts of iron, aluminum, titanium, and silicon removed from the ash were calculated based on analyses of the nonreacted residues.

Finally thermodynamic calculations were done for compounds that approximated those in fly ash and an extensive literature review of chlorination reactions similar to those of fly ash and chlorine was conducted. The results and information from the measurements, experiments, calculations, and literature review were considered and conclusions were reached concerning the reaction rate and final conversion limitations. Also, some general facts and ideas, developed during the review of the information, are noted and could be useful for future investigations of the chlorination of fly ash.

THERMODYNAMIC CONSIDERATIONS

Many thermodynamic studies on gas-solid reaction systems similar to that of fly ash and chlorine have been published (11, 24, 33, 35, 39). For such studies to be useful as a predictive tool, the element and compound compositions and their availability in the solid must be known as a starting point. It must be known how the elements are combined and whether they are accessible. If the experimental system to which the thermodynamic calculations are to apply is a flow system, it must be assumed that equilibrium is established in the stagnant gas layer surrounding each particle. Also, the kinetics of the reaction and the diffusion of the reactant gases to the solid surface must be fast. Assuming that both the kinetics and mass transfer are fast is like wanting the best of both. It is quite likely that if the kinetics are very fast, that the mass transfer will not be fast enough to keep an equilibrium concentration of reactant gases at the solid surface. Also, due to the complexity of the calculations, simplifying assumptions must be made. For example, it could be assumed that the activity of all solids and liquids is one. Any such assumption potentially limits the accuracy of the results.

Hence, thermodynamic studies should be treated equal to what they are, initial approximations. The information can be used as a starting point for investigation of a gas-solid system but no great significance should be attached to the results. If the free energy change for a given reaction is large and negative, it is safe to assume that the reaction will occur.

Table 1 lists potential reactions and their corresponding Gibb's free energy and enthalpy changes for the chlorination of fly ash. It was assumed that even though fly ash consists mostly of alumina-silica glasses, that alumina and silica treated separately would approximate the reactivity of the glasses. All enthalpy and Gibb's free energy changes were calculated using data from Barin and Knacke (5b). For reactions 1-19, there is a common basis of three moles of chlorine being reacted. Also, no calculations were made for reactions occurring above 800°C for systems in which phosgene was used because it will dissociate into carbon monoxide and chlorine at these temperatures.

The first 14 reactions, those in which carbon is used as the reductant, have smaller negative free energy changes than those in which either carbon monoxide or phosgene are used. Also, for temperatures of 600°C and greater, phosgene chlorination reactions have higher negative free energy changes than do corresponding carbon monoxide reactions. If free energy changes for reactions 1, 6, 9, and 12 or 3, 7, 10, and 13 or 5, 8, 11, and 14 are compared within their groups for the temperatures between 700 and 1000°C, it is seen that the materials listed in order of decreasing reactivity are Fe_2O_3, TiO_2, Al_2O_3, and SiO_2.

Free energy changes for reactions 15-18 indicate that none of the materials can be chlorinated directly with chlorine. However, the negative free energy changes of reaction 19 indicate that it is possible to directly chlorinate a material containing Fe_2O_3 if it is first reduced to FeO. This prereduction could be applicable to fly ash as a method to remove the iron prior to chlorination of alumina.

The free energy changes for reaction 20 indicate that the iron

Table 1. Free energy and enthalpy values as a function of temperature for the chlorination of selected metal oxides found in fly ash

Reaction number	Reaction
1	$Fe_2O_3(S) + 3C(S) + 3Cl_2(g) = 2FeCl_3(g) + 3CO(g)$
2	$2FeO(S) + 2C(S) + 3Cl_2(g) = 2FeCl_3(g) + 2CO(g)$
3	$Fe_2O_3(S) + 3CO(g) + 3Cl_2(g) = 2FeCl_3(g) + 3CO_2(g)$
4	$2FeO(S) + 2CO(g) + 3Cl_2(g) = 2FeCl_3(g) + 2CO_2(g)$
5	$Fe_2O_3(S) + 3COCl_2(g) = 2FeCl_3(g) + 3CO_2(g)$
6	$Al_2O_3(S) + 3C(S) + 3Cl_2(g) = 2AlCl_3(g) + 3CO(g)$
7	$Al_2O_3(S) + 3CO(g) + 3Cl_2(g) = 2AlCl_3(g) + 3CO_2(g)$
8	$Al_2O_3(S) + 3COCl_2(g) = 2AlCl_3(g) + 3CO_2(g)$
9	$3/2\ TiO_2(S) + 3C(S) + 3Cl_2(g) = 3/2\ TiCl_4(g) + 3CO(g)$
10	$3/2\ TiO_2(S) + 3CO(g) + 3Cl_2(g) = 3/2\ TiCl_4(g) + 3CO_2(g)$
11	$3/2\ TiO_2(S) + 3COCl_2(g) = 3/2\ TiCl_4(g) + 3CO_2(g)$
12	$3/2\ SiO_2(S) + 3C(S) + 3Cl_2(g) = 3/2\ SiCl_4(g) + 3CO(g)$
13	$3/2\ SiO_2(S) + 3CO(g) + 3Cl_2(g) = 3/2\ SiCl_4(g) + 3CO_2(g)$
14	$3/2\ SiO_2(S) + 3COCl_2(g) = 3/2\ SiCl_4(g) + 3CO_2(g)$

Table 1. Continued

Reaction number	Reaction
15	$Fe_2O_3(S) + 3Cl_2(g) = 2FeCl_3(g) + 3/2\ O_2(g)$
16	$Al_2O_3(S) + 3Cl_2(g) = 2AlCl_3(g) + 3/2\ O_2(g)$
17	$3/2\ TiO_2(S) + 3Cl_2(g) = 3/2\ TiCl_4(g) + 3/2\ O_2(g)$
18	$3/2\ SiO_2(S) + 3Cl_2(g) = 3/2\ SiCl_4(g) + 3/2\ O_2(g)$
19	$2FeO(S) + 3Cl_2(g) = 2FeCl_3(g) + O_2(g)$
20	$Fe_2Cl_6(g) = 2FeCl_3(g)$
21	$Al_2Cl_6(g) = 2AlCl_3(g)$
22	$2Al_2O_3(S) + 3SiCl_4(g) = 4AlCl_3(g) + 3SiO_2(S)$
23	$C(S) + 1/2\ O_2(g) = CO(g)$
24	$CO(g) + 1/2\ O_2(g) = CO_2(g)$
25	$C(S) + CO_2(g) = 2CO(g)$

Table 1. Continued

Kcal/G-mole									
ΔG_{600}[a]	ΔH_{600}	ΔG_{700}	ΔH_{700}	ΔG_{800}	ΔH_{800}	ΔG_{900}	ΔH_{900}	ΔG_{1000}	ΔH_{1000}
- 106.9	- 8.4	- 118.3	- 10.2	- 129.3	- 12.1	- 140.1	- 13.1	- 150.9	- 14.4
- 101.0	- 47.4	- 107.1	- 48.2	- 113.1	- 49.2	- 119.0	- 50.3	- 124.8	- 51.4
- 114.6	- 131.7	- 118.4	- 132.9	- 116.8	- 134.1	- 115.1	- 134.4	- 113.5	- 135.0
- 109.4	- 129.5	- 107.1	- 130.0	- 104.7	- 130.6	- 102.3	- 131.2	- 99.8	- 131.8
- 126.7	- 54.4	- 135.0	- 56.1	- 143.0	- 57.9	—	—	—	—
- 58.6	39.1	- 69.8	38.4	- 80.8	37.4	- 91.7	36.4	- 102.7	34.3
- 71.3	- 84.1	- 69.8	- 84.4	- 68.2	- 84.6	- 66.7	- 84.9	- 65.2	- 86.2
- 78.3	- 6.8	- 86.4	- 7.6	- 94.5	- 8.4	—	—	—	—
- 90.2	- 15.1	- 98.8	- 15.8	- 107.2	- 16.4	- 115.7	- 20.3	- 124.1	- 18.0
- 102.9	- 138.4	- 98.8	- 138.5	- 94.7	- 138.5	- 90.7	- 141.6	- 86.6	- 138.6
- 109.9	- 61.1	- 115.5	- 61.7	- 121.0	- 62.2	—	—	—	—
- 60.5	- 10.1	- 68.6	- 9.6	- 76.6	- 8.7	- 84.5	- 7.8	- 92.5	- 7.7
- 73.2	- 309.4	- 68.7	- 312.0	- 64.1	- 314.1	- 59.5	- 316.4	- 55.0	- 319.4
- 80.3	- 232.2	- 85.3	- 235.2	- 90.3	- 237.9	—	—	—	—

---

[a] All subscripted numbers are temperatures in °C.

Table 1. Continued

Kcal/G-mole									
ΔG_{600}	ΔH_{600}	ΔG_{700}	ΔH_{700}	ΔG_{800}	ΔH_{800}	ΔG_{900}	ΔH_{900}	ΔG_{1000}	ΔH_{1000}
28.6	71.4	23.6	69.9	18.9	68.5	14.4	67.9	9.8	66.8
77.0	119.0	72.2	118.5	67.4	118.0	62.8	117.5	58.1	115.6
45.0	64.6	43.1	64.4	41.0	64.2	38.8	60.8	36.7	63.2
75.1	- 106.4	73.3	- 109.1	71.6	- 111.5	70.0	- 114.0	68.3	- 117.5
- 10.6	5.9	- 12.5	5.2	- 14.3	4.5	- 16.0	3.8	- 17.6	2.8
5.4	33.0	2.2	32.6	- 0.9	32.2	- 3.9	31.8	- 7.0	31.4
0.3	27.5	- 2.8	27.0	- 5.9	26.7	- 8.9	26.3	- 11.9	24.8
3.9	450.8	- 2.2	455.3	- 8.3	459.0	- 14.4	462.9	- 20.4	466.2
- 45.2	- 26.6	- 47.3	- 26.7	- 49.4	- 26.9	- 51.5	- 27.0	- 53.6	- 27.1
- 49.4	- 67.7	- 47.3	- 67.6	- 45.2	- 67.6	- 43.2	- 67.5	- 41.1	- 67.3
4.2	41.1	0.0	40.9	- 4.2	40.7	- 8.3	40.4	- 12.5	40.2

chloride monomer form is favored over the dimer for temperatures of 800°C and higher. The same is true for aluminum trichloride in reaction 21 for temperatures of about 650°C and higher. Also, reaction 22 free energy changes show that for temperatures above 675°C, silicon tetrachloride will chlorinate alumina. The free energy changes for reaction 25 indicate that at about 700°C, the equilibrium between CO_2, C, and CO shifts toward CO. This is very important because if a reaction system in which solid carbon is used as the reductant were operated below 700°C, the carbon usage could possibly be cut in half. Enthalpy changes of the reactions 1-14 are all negative except for reaction 6 in which alumina is chlorinated with C and Cl_2. If fly ash were composed of the materials used in these reactions, it could be stated that the overall reaction would be exothermic.

LITERATURE REVIEW

A great deal of research has been done during the past three decades on the chlorination of a wide variety of substances. Often the research was intended to help explain a system and allow for development of a commercial process or to improve an existing process. A cross section of the chlorination experiments that might give results pertinent to fly ash chlorination involved the following materials: bauxite (19, 29, 31, 34, 36, 43), ilmenite (13, 18, 26, 42, 43), rutile (6, 37, 41, 49), aluminous clays (20, 31, 32), and pure components (1, 2, 11, 15, 16, 17, 36). This group will be collectively referred to as primary reactants. The experiments on each class of substances will be reviewed by mentioning the optimum operating conditions, trends with respect to changes in conditions, reaction limitations, and possible reaction mechanisms.

It must be stressed that only optimum chlorination conditions and conversions will be noted for a given set of experiments. Many variables could be important in determining conversions and reaction rates. Those which were easy to alter were optimized or at least placed at their upper limit. However, there are some variables that are not easy to change. Two examples are particle size and surface area. It is difficult to crush an ore down to - 200 mesh. Also, once an ore has a given surface area for a certain desired particle size range, it is hard to change it. Rutile and ilmenite are good examples of such ores. Bauxite and clays have an advantage over rutile and ilmenite because, in their mined state, they contain a large amount of hydrated water. When the ore is heated, the water vaporizes and leaves a porous, high-surface area material. Therefore, in reviewing a set of experiments, it should be understood that if, for example, the chlorine flow rate is not mentioned, it is because the rate was held at such a level that it was not limiting the conversion or reaction rate.

Chlorination of Bauxite

The bauxites chlorinated were low-grade, having weight percent compositions of 1-10 silica, 50-60 alumina, 1-5 titania, and 5-10 iron oxides (29). The majority of the alumina present was in the form of alumina trihydrate (36). Prior to chlorination, the bauxite was calcined at temperatures up to 1000°C (19) to remove the water. The expulsion of water left a very porous, high surface area material. The surface areas ranged from 40 M^2/g (31) to 80 M^2/g (36).

After calcining, the bauxite was sometimes pretreated to remove the nonaluminum contaminants (19, 29, 36). Iron oxides were judged the most undesirable constituents, so pretreatment schemes usually worked to remove these oxides. Milne and Wibberley (36) reacted bauxite ground to - 100 + 200 mesh with HCl gas at temperatures not exceeding 800°C and reduced the bauxite iron oxide content to 0.3 weight percent. Another iron removal scheme involved the reaction of - 4 mesh bauxite particles with a 35:65 mixture of SO_2:CO for 15 minutes at 700°C (19). This reaction converted the iron oxides to ferrous sulfide. The FeS was then reacted for 10-20 minutes with chlorine at 750°C to give iron oxide levels of 0.1-0.3 weight percent in the bauxite.

Carbon reduction of iron oxides to elemental iron was also considered. Bauxite of - 80 mesh was mixed with wood charcoal in the ratio of 75 grams bauxite to 20 grams charcoal and then heated for 2.5 hours at 900°C (29). This roasted material was washed with dilute hydrochloric acid solution. The amount of iron oxide extracted was calculated to be 30 percent. The latter method was much slower and did not lower the iron oxide level as much as the two previously mentioned schemes.

In general, chlorinations were done using several different combinations of reducing and chlorinating agents. The most common reductant-chlorinator pairs, to be referred to as secondary reactants, were: $C\text{-}Cl_2$, $CO\text{-}Cl_2$, and $COCl_2$. Phosgene ($COCl_2$) combines the reductant and chlorinator into one molecule.

Several investigations of the chlorination of bauxite using the $C\text{-}Cl_2$ combination have been reported (29, 31, 36, 43). Bauxite ground to - 100 + 200 mesh and having a surface area of 80 M^2/g was pyrolytically coated with carbon using methane in a fluidized-bed reactor at 900°C (36). The optimum range of carbon deposition on the bauxite was determined to be 25-27 weight percent. Chlorination reactions were done using small samples of the coated bauxite on a thermobalance. A sample could be chlorinated at 800°C to give 80 percent conversion in 8 minutes. However, this was the upper limit of conversion even if excess carbon was present. A multistage fluidized-bed process in which pyrolytic carbon coating and chlorination cycles were repeated on the same sample, converted more than 90 percent of the bauxite within two cycles.

Another set of bauxite chlorination experiments involved reaction of bauxite-charcoal briquetts with chlorine in a vertical-flow reactor

(29). The effects of temperature, bauxite to charcoal ratio, binding agent, and catalyst were determined to be 980°C, 100:45, sulfite liquor, and silicic acid, respectively. Using this set of conditions, the conversion was nearly complete. The final bauxite conversions and the reaction rates both increased as the four above parameters increased up to the optimum. The required reaction period, however, was five hours.

In research on the Toth process, bauxite was chlorinated using coke and chlorine. Bauxite was calcined, mixed with coke, and chlorinated in a fluidized-bed reactor in contact with a stream of chlorine gas at 925°C. No specifics concerning yields were given (43).

Landsberg (31) chlorinated bauxite using carbon, carbon monoxide, and chlorine. The bauxite was calcined at 1000°C prior to chlorination. The BET surface area was 40 M^2/g. Results were given for experiments done using a 50:1 ratio of bauxite to carbon chlorinated with a 50:50 mixture of CO and Cl_2 at 600°C. The elemental compositions of the bauxite were followed for a one-hour chlorination period. After 94 percent iron, 85 percent titanium, 35 percent alumina, and 45 percent silica were converted to chlorides. The purpose of the experiment was to determine if impurities, iron, titanium, and silica, could be removed at lower temperatures (600°C) prior to chlorination of the alumina at higher temperatures (700°C and up). Obviously, the loss of alumina was too high and the removal of impurities too low to make the process attractive. Other experiments were done using only a 50:50 mixture of CO and Cl_2 without any carbon present. The conversion of bauxite was 75 weight percent at 600°C for a one-hour chlorination period.

Two factors were important in the bauxite chlorinations. They were calcining temperature and contact between the carbon and the bauxite. Milne and Wibberley (36) stressed that the physical form of the bauxite prior to chlorination was very important. Two properties altered by high calcining temperatures were the surface area and the chemical composition (36). When the bauxite was calcined at 800°C or less (36), the surface area was 80 M^2/g, however, when heated to 1000°C (31), the area was given as 40 M^2/g. Landsberg (31) also noted that the reaction rate slowed because of the presence of unreacted alpha-alumina. The formation of alpha-alumina was attributed to high calcining and chlorination temperatures.

The effect of carbon-bauxite contact is evident if the reaction conversions and reaction times are compared for the experiments mentioned. The pyrolytically-carbon coated bauxite reacted most rapidly, whereas the briquetted carbon-bauxite mixture was the slowest. Prior to pyrolytic coating, the bauxite had a surface area of 80 M^2/g, but following the coating, giving a sample of 25 weight percent carbon, the surface area was 25 M^2/g (36). The carbon was deposited within the pores, giving maximum carbon-bauxite contact.

In the briquetted system, the bauxite was mixed with carbon and the mixture then pressed into briquettes using sulfite liquor as the binding agent (29). Here the carbon would only be in contact with the external surface area of the bauxite. The $CO-Cl_2$ chlorination rates fell between those for the two systems already mentioned. It was suggested that the $CO-Cl_2$ system reacted faster than the briquetted system because the CO and Cl_2, both being gases, could travel to the reaction sites within the bauxite.

Landsberg (31) calcined bauxite at several temperatures to produce bauxites with a range of surface areas. He found that for comparable chlorination conditions, the higher the initial surface area, the greater the reaction rate. Therefore, high bauxite surface areas were important, especially for the pyrolytic and CO-Cl_2 systems. In both cases, the higher the surface area, the greater the contact between reactants and the higher the reaction rate.

Effects of binding agent and catalyst in the briquetted system were also studied (29). The best combination was sulfite liquor for the binding agent and silicic acid for the catalyst. The reaction rate increases were attributed to the formation of reaction intermediates which decayed to another form after chlorinating some of the bauxite. An example was the use of silicic acid as a catalyst. Silicon tetrachloride was formed and then reacted with alumina to give aluminum trichloride and silicon dioxide (29).

Chlorination of Clays

The clays chlorinated had a wide variation in composition. The weight percent composition ranges were 24-52 SiO_2, 24-45 Al_2O_3, 0.5-3 Fe_2O_3, and 1-2 TiO_2 (20, 31, 32). The composition differences between the clay and low-grade bauxite were that the iron oxide, titania, and alumina concentrations were lower, and the silica concentration higher, in the clays.

The effects of grain size, chlorine flow rate, reaction period, and temperature were investigated during the chlorination of two Egyptian clays (20). All chlorinations were done using solid carbon as the reductant. The optimum grain size for one clay was 70 mesh and 100 mesh for the other. Chlorine flow rate had little effect on conversion. However, the final conversion and reaction rate increased with either temperature or reaction period. The optimum carbon content was determined as four times the amount necessary to convert all of the oxygen to carbon dioxide. When using the optimum clay particle sizes and carbon content, chlorinations at 1000°C for seven hours gave alumina conversions of 90 weight percent.

Landsberg (32) studied the effects of temperature, catalyst concentration, and chlorination period on the conversion of clays. In one series of experiments solid reductants were used; reductants were graphite, coke, and charcoal. The catalyst used in these experiments was sodium chloride. The highest conversion of 63 weight percent clay was achieved when a 10:2:1 ratio of clay to charcoal to sodium chloride mixture was chlorinated in a thermal balance reactor at 625°C. The reaction time was 40 minutes.

Clay chlorinations were also conducted using gaseous reductants. Landsberg (31) chlorinated clay using a stream of either a 0.4:0.4 atmosphere partial pressure mixture of CO and Cl_2 or else 0.8 atmospheres of phosgene. The 0.2 atmosphere remainder was an inert gas such as argon. The reaction rate of phosgene at 700°C was comparable to the rate of CO-Cl_2 at 1100°C. Above 800°C, the phosgene gave results similar to the CO-Cl_2 system due to dissociation into CO and Cl_2.

It was shown that between 600 and 900°C, the reaction rate depended directly on the partial pressure of CO and Cl_2. Clay chlorinated at 700°C with CO and Cl_2 for two hours gave weight percent elemental conversions of 12, 23, 45, and 90 for Si, Al, Fe, and Ti, respectively. The reaction rates were about ten times higher when phosgene was used.

Landsberg (32), in a more recent study of the chlorination of clays, used a CO-Cl_2 system with sodium chloride as a catalyst. The experiments were conducted on a thermal balance instrument. A mixture of 10:1 parts clay to NaCl was chlorinated using a 50:50 mixture of CO and Cl_2 at 625°C. The conversions were 90 weight percent aluminum and less than 5 weight percent silicon for a 55-minute period. This is a desirable result due to the low conversion of silicon. The sodium chloride addition was cited as the reason for the low silicon conversion. Apparently, the sodium chloride reacted with the alumina to form sodium aluminum chloride which made the remaining aluminous material more reactive to chlorine (31).

The physical state of the clay was closely followed during one set of experiments (31). Initially, the surface area was 12 M^2/g. After a 12-hour chlorination at 900°C, the surface area had increased to 75 M^2/g. Microscopic examinations showed that the clay sintered during the chlorination to give a large number of very small particles.

Comparison of Bauxite and Clay Chlorination

The clay and bauxite chlorinations gave similar results. In both cases, gaseous reactants were much more effective chlorinators. Also, the reactions were shown to be very dependent on temperature. As the temperature increased, the conversions and reaction rates increased.

One important difference was the change in surface area with conversion. As the bauxite conversion increased, the surface area decreased (36). The opposite was true for clays (31). This could possibly be explained by considering initial compositions. As was mentioned, clays have more silica and less alumina, iron oxides, and titania. Bauxite has a high surface area and therefore, an intricate pore structure; the silica present is said to be nonreactive quartz (31). If, as the bauxite chlorination proceeded, the alumina, iron oxides, and titania were chlorinated to a large extent, leaving the nonreactive silica, the surface area would greatly decrease. In the case of clays, the lower initial surface area and higher concentration of silica indicates that the iron oxides, titania, and alumina were possibly mixed with and buried in the silica. When chlorinated, these more reactive constituents would be extracted, leaving the silica in a somewhat more porous form.

The carbon to clay contact was considered to be important (32). Graphite, coke, and charcoal were used in separate experiments as reductants in the chlorinations of clay. Charcoal was shown to be the most effective reductant. Its higher surface area, resulting in greater clay-charcoal contact, was given as the reason for higher conversions and reaction rates. However, most surface area is really internal surface area, so for the clay to have increased contact with the charcoal, clay particles would have to enter the charcoal pores. This is very unlikely. Another explanation may be that the charcoal, having an extremely rough surface, allows clay particles to drop into its crevices.

A better example of the effect of carbon-clay contact was found in research of the chlorination of Egyptian clays (20). As the clay particle sizes decreased and the carbon content increased, the conversions increased. Both effects contribute to increasing the clay-carbon contact. These data showed a limit for particle sizes, however, because, as the size became extremely small, chlorine flow and dispersion were hindered.

Chlorination of Ilmenite

In the bauxite and clay chlorination, the recovery of aluminum was the prime objective. Now, two titanium ores, ilmenite and rutile, will be discussed. Ideally, ilmenite is $FeO-TiO_2$ and rutile is TiO_2. The rutile form is more desirable, and therefore, several beneficiation studies have been carried out to remove the iron from ilmenite (13, 42, 43). The methods were quite successful in lowering the iron content and, as an added advantage, the beneficiated ilmenite had a much higher surface area.

Two studies included experiments on the chlorination of raw ilmenite (18, 26). The average weight percent composition of the raw ilmenite ore was 60 TiO_2, 32 Fe_2O_3, 1 Al_2O_3, and 1 SiO_2 (18, 26). There is a large difference between this composition and those of clays and bauxite. The alumina and silica are not significant in the ilmenite whereas, the iron oxides and titania concentrations are much greater than those found in the bauxite and clays. As the ilmenite formula indicates, the iron oxides should be in the FeO form. Analyses determined, however, that most of the iron oxides were in the Fe_2O_3 form. Thermodynamically, the Fe_2O_3 is much less reactive with chlorine than the FeO (26).

Ilmenite, ground to - 200 mesh and mixed with charcoal, was chlorinated in a fixed-bed reactor (26). The sample size was 5 grams, the chlorine flow rate 4 liters per hour, the ilmenite to charcoal ratio 100:30, the chlorination period one hour, and the temperature range was 400-600°C. Using the above conditions at a temperature of 500°C, weight percent conversions of both titania and iron oxides of about 90 percent were achieved. Catalysts were also tested. Ilmenite was chlorinated using the same conditions at 400°C and 0.05 grams of cerium oxide was added. The TiO_2 and Fe_2O_3 weight percent conversions were 81.3 and 89.0, respectively. No explanation was given as to why the catalyst enhanced the reaction rate.

The Bureau of Mines (Harris, et al., 18) has investigated fluidized-bed chlorination of ilmenite. Petroleum coke was used as the reductant. The ilmenite was ground to 90 percent - 325 mesh and the coke to - 20 + 100 mesh. A carbon to ilmenite mole ratio of 3.8 was used. The coke-ilmenite mixture and chlorine were continuously fed to the reactor.

The conversion was temperature dependent and increased with temperature to the upper limit if 1150°C. With a chlorine flow of 18.0 liters per minute, a solids feed of 30 grams per minute, and a temperature of 1150°C, the TiO_2 weight percent conversion was 97.4. This was also reported as a 95.3 percent conversion of the reactor solids fed during the test period.

In the first set of ilmenite experiments (26), the charcoal to ilmenite mole ratio was important. As this ratio increased, the reaction rate increased. However, the chlorine flow rate had little effect on the rate. This would indicate that the chlorine availability was not limiting the reaction, but that the charcoal was. In comparing the fixed-bed systems, it should be noted that the temperature was one-third as high as the fixed-bed experiments. Also, the particle size was smaller in the fluidized-bed case. The temperature and particle size conditions may explain the higher conversions of the fluidized-bed system.

One very important parameter, the ilmenite surface area, was not determined during the experiments. As the thermodynamics indicate, wuestite (FeO) can react directly with chlorine without carbon present. Therefore, the carbon may have served as an oxygen sink, used only to carry away the oxygen that was displaced from the FeO on the ilmenite surface. If this were the case, the amount of ilmenite surface area may have directly limited the reaction rate.

Chlorination of Rutile

The iron content is much lower and the titania much higher for rutile when compared to ilmenite. The weight percent ranges for the rutile ores chlorinated were: 94-97 TiO_2, 0.4-0.6 Fe, and minute quantities of Al, Si, V, and Zr (6, 13, 49). Surface area measurements indicated that rutile particles were not porous (37). This being the case, most reactions would occur on the outer surface until a pore structure was developed.

Vijay, et al. (49) used fluidized-bed chlorinations to determine the effects of temperature, reaction period, chlorine flow rate, particle size, and rutile to coke ratio on the conversion of rutile. The rutile and petroleum coke were ground to - 60 + 200 and - 20 + 48 mesh, respectively. With a chlorine flow of 40 liters per hour, a coke to rutile ratio of 1:1, and a temperature of 900°C, the highest conversion, 68 weight percent, was obtained for a 15-minute chlorination. The reaction rate increased with increasing temperature, but was not affected by chlorine flow rates ranging from 30-50 liters per hour.

Another set of fluidized-bed experiments (37) also dealt with the chlorination of rutile using petroleum coke and chlorine. The particle size distribution was - 80 + 100 mesh. The results were only given in terms of fits to reaction models, making it difficult to determine what the conversions were for a given set of conditions. Also, some $CO\text{-}Cl_2$ chlorinations of rutile were conducted using conditions comparable to those of the chlorine-coke system. The reaction rates were found to be 19 times faster for the chlorine-coke system.

Bergholm (6) reported on an extensive study on the effects of operating conditions on the conversion of rutile. One set of experiments was run to examine the effect of the distances between the solid reductant and the rutile particles. A tablet of - 200 mesh rutile was placed on top of an equal-sized tablet of char in a quartz boat. Grooves of known depth were cut into the rutile prior to exposing the tablets to chlorine at 800°C. After a three-hour chlorination period, the rutile surface was microscopically examined. Grooves that had been cut deeper than about 200 microns showed no sign of reaction; however, any surface that was less than 200 microns from the char, was roughened, indicating that reaction had occurred. Direct contact between the rutile and char was not necessary.

Using the same reactor system, tablets made from a 100:30 weight ratio mixture of rutile to carbon were chlorinated (6). The tablets were reacted using various mixtures of chlorine, carbon monoxide and dioxide, and argon. Temperature and particle sizes were important variables in the reactions. The temperature was varied from 700 to 800°C and the particle size range was - 48 + 200 mesh. The optimum conversion of 4.2 weight percent of the rutile sample per minute was obtained for tablets consisting of - 140 + 200 mesh rutile and char particles in a stream of pure chlorine at 695°C. The rates of conversion for these runs depended strongly on the chlorine concentration and flow rate.

In another set of experiments (6), rutile ground to - 140 + 200 mesh was mixed with metallurgical coke of - 200 mesh and pressed into tablets. The tablets, having a rutile to coke ratio of 50:7, were chlorinated in a quartz boat. Also, an unpelleted mixture with a 3:1 ratio of rutile to coke was chlorinated in both a fixed- and fluidized-bed reactor. For the powder sample experiments, the rutile and coke particle sizes were - 60 + 100 mesh and - 30 + 60 mesh, respectively.

For the tablet chlorinations, the highest reaction rate of 4.5 rutile sample weight percent per minute was obtained for a chlorine flow of 40 liters per hour at 680°C. The same chlorine flow rate dependence was observed as in the previous tablet chlorinations. The chlorination rate for the powder, fixed-bed system, was a strong function of temperature. The rate increased with temperature up to 1010°C. The tablet chlorination rate was ten times faster than the powder fixed-bed system for comparable reaction conditions. The fluidized-bed system was not well-tested and very little data were given.

Morris and Jensen (37) reported on a set of experiments in which rutile was chlorinated using chlorine and gaseous reductants. A fluidized-bed reactor was charged with 200 grams of rutile, - 80 + 100 mesh, and chlorinated under a stream of CO and Cl_2. The reaction rates depended on temperature and on the partial pressures of chlorine and carbon monoxide. The rate increased with temperature, and as the product of the partial pressures of CO and Cl_2 was increased. A conversion of 43 weight percent rutile was obtained for a 2.3-hour chlorination at 1054°C with a 50:50 carbon monoxide:chlorine feed ratio.

Dunn (13) beneficiated ilmenite with Cl_2 and CO to produce rutile. No particle sizes or surface areas were given but the surface area of the beneficiated ilmenite was expected to be higher than that of natural rutile since the iron oxides were removed from throughout the ilmenite. Both fixed- and fluidized-bed chlorinations were done. Comparable results were obtained for both reactor geometries.

Both beneficiated ilmenite and rutile ores were chlorinated using either CO-Cl_2 or phosgene (13). For the CO-Cl_2 system, the chlorination rate was directly dependent on the CO and Cl_2 feed concentrations. An optimum reaction rate was obtained when a 50:50 ratio of CO and Cl_2 at 900°C was used. The reaction rate for beneficiated ilmenite was 2.5 TiO_2 sample weight percent per minute. This removal rate was constant until almost total conversion had taken place. The chlorination rate for the same material using phosgene at 530°C was 8 weight percent per minute. As has been mentioned previously, the phosgene chlorination rate will resemble that of a CO-Cl_2 system when at temperatures above 800°C. The beneficiated ilmenite reacted about ten times faster than the rutile. Since the only known difference between the two was the surface areas, apparently the higher surface area of beneficiated ilmenite was the reason for the higher reaction rate.

Bergholm (6) chlorinated rutile, - 40 + 100 mesh, in a quartz boat with an equimolar flow of CO and Cl_2. This gas composition at a temperature of 1000°C gave an optimum rate of reaction of 0.13 weight percent sample conversion per minute. The reaction rate was sensitive to temperature and carbon monoxide feed composition, but the chlorine feed concentration was not extremely important.

In summary, two factors appeared to greatly limit conversions. They were the rutile surface area and rutile-carbon proximity. Several experimental results indicated that the rutile surface area was important.

Three of the investigations (6, 13, 37) indicated that the reaction rate increased as the rutile particle sizes decreased. As particle size decreases, the specific surface area of the sample increases. Another indication of surface area limitations is evident if the chlorination rates for the beneficiated ilmenite and rutile are compared (13). The beneficiated ilmenite, having a higher surface area, chlorinated much faster than the rutile. In two instances (49, 37) data were fit to shrinking-unreacted core reaction models. As the name indicates, these models fit data for particles that are nonporous and react on the external surface only.

Several investigators have indicated that the rutile-carbon distances or proximity are important. The experiments in which separate rutile and char tablets were chlorinated gave the best indication that the distances between the carbon and rutile particles are important (6). In addition, the much higher reaction rates of the rutile-carbon tablets, compared to powder mixtures, indicated that rutile-carbon proximity is important. The ratio of rutile to carbon had an influence on reaction rates. This effect may also be interpreted in terms of rutile-carbon proximity. The more carbon particles present, the greater the chance that one will be in close proximity to a rutile particle. Therefore, a 1:1 rutile to carbon mixture as compared to a 10:3 mixture gave much higher reaction rates.

Chlorine flow rates also affect the reaction rates. However, the only time chlorine flow effects were mentioned was when compressed tablets were chlorinated (6). Usually, an increase in reaction rate with gas flow rate indicates mass transfer is controlling. Since no such limitations were mentioned for powder chlorinations, it is likely that the diffusion of gaseous reactants into and products out of the tablets caused the mass transfer limitations. Two other rate dependencies are evident; the effects of temperature and gaseous reactant concentration. Table 1 indicates that all of the Fe_2O_3 and TiO_2 reduction-chlorination reactions are exothermic. Therefore, if the system were thermodynamically controlled, an increase in temperature should decrease the reaction rates. Since this was contradicted by increases in reaction rates with temperature, apparently the higher temperatures serve to enhance the kinetics of the system. The higher reaction rates as a result of increases in gaseous reactant concentrations is probably also due to enhanced kinetics.

Chlorination of Pure Components

Alumina

Alumina was usually chlorinated in an effort to explain data obtained from bauxite chlorinations. The reaction systems used were C-Al_2O_3-Cl_2, CO-Al_2O_3-Cl_2, and $COCl_2$-Al_2O_3. Two investigations (2, 31) dealt with the chlorination of alumina using carbon and chlorine. Landsberg (31) covered small rectangular compacts of gamma-alumina with - 325 mesh carbon and reacted them under a stream of chlorine. The reaction rates ranged from 0.042 weight percent per minute at 1075°C to 0.0045 weight percent per minute at 890°C. When the same C-Al_2O_3 system was reacted under a mixture of 0.8 atmosphere chlorine and 0.2 atmospheres oxygen, the reaction rate was 0.5 weight percent per minute at 800°C and 0.001 weight percent per minute at 560°C. The oxygen was postulated to react with the carbon to form CO; the CO then served as the reductant for the reaction of alumina with chlorine.

Alder (2) chlorinated alumina using three different forms of solid reductant and chlorine. Solid carbon reductants were introduced by pyrolytically coating the alumina, by carbonizing a mixture of glucose and alumina, and by mixing alumina with soot. The chlorination experiments were conducted on a thermal microbalance. Alumina with a surface area of 124 M^2/g was obtained by dehydrating a Bayer trihydrate at 800°C. The alumina was then ground to an average particle size of 63 microns. Alumina-carbon samples were chlorinated over a temperature range of 670 to 810°C with pure chlorine. The carbon to alumina ratios for the pyrolytic carbon, glucose, and soot systems were 0.23, 0.26, and 0.26, respectively.

For chlorinations at 800°C, the weight percent conversions of alumina and reaction periods were 100 percent complete after 2.5 minutes for the pyrolytic carbon system, 50 percent complete after 7.5 minutes for the glucose system, and 45 percent complete after 12 minutes for the soot system. For the soot and glucose systems, the conversions given were the upper limits, the reactions had essentially stopped. The conversions of alumina for these alumina-carbon systems were temperature dependent, with the pyrolytic carbon-alumina system being especially sensitive. At 800°C, after 2.5 minutes, the conversion was complete, however, at 670°C, after 12 minutes, the conversion was only 28 percent complete.

The alumina used had a surface area of 124 M^2/g, but, after it was pyrolytically coated, the surface area was only 13 M^2/g. Even though the pyrolytically coated alumina had by far the lowest surface area, it was the most reactive. This indicates that it is the contact area between carbon and alumina which effects reactivity and that the high alumina surface area is important only because more carbon can be deposited in contact with the alumina.

Landsberg (31) chlorinated both alpha and gamma alumina using a 0.4, 0.4, and 0.2 atmospheres partial pressure mixture of Cl_2, CO, and argon, respectively. The reaction rate of gamma-alumina was 0.8 weight percent per minute for temperatures of 400-800°C. However, the conversion rate for alpha-alumina increased from 0.001 weight percent per minute at 400°C to 1.3 weight percent per minute at 1100°C. When gamma-alumina was chlorinated to near completion, only alpha-alumina, which probably formed during the calcining of the trihydrate to alumina, remained. The reaction rate depended on the CO and Cl_2 feed concentrations for temperatures between 250 and 600°C. However, above 600°C, the reaction seemed to be limited only by mass transfer effects.

Alder (1) chlorinated alumina using CO and Cl_2, monitoring the reaction with a thermal microbalance. Dehydrated aluminum hydroxide was used for the chlorinations. Dehydration at 800°C gave alumina with a surface area of 180 M^2/g, whereas, a dehydration temperature of 400°C gave a surface area of 280 M^2/g. Consistent with the surface area differences, the reaction rate for the material dehydrated at 400°C was 2.3 times faster than that dehydrated at 800°C. The reaction was temperature dependent over the range of 400-600°C. However, between 600 and 800°C, the conversions were equal at 80 percent completions for

40-minute chlorinations which may indicate that mass transfer, rather than kinetics, limited the reaction.

The physical characteristics of the alumina were checked at different degrees of conversion. As the conversion increased, the surface area decreased but the particle diameter remained constant. With reaction, the interior pore structure is destroyed which hollows out the particles. The total surface area, therefore, decreases while the particles maintain approximately the same outer shape.

Chlorinations of alumina using phosgene were very fast (2). A conversion of about 90 weight percent was reported for a 5-minute chlorination at 512°C. For a 2-minute chlorination at 699°C, the conversion was complete. For a $CO-Cl_2$ system at comparable temperatures, the weight percents reacted were 33 and 68, respectively, with 25-minute reaction times.

As in the case of bauxite, clays, ilmenite, and rutile, surface area and carbon proximity were also important in the chlorination of alumina. High surface areas enhanced the reaction rate of both the $C-Al_2O_3-Cl_2$ and $CO-Al_2O_3-Cl_2$ systems, especially in the case of pyrolytically coated carbon-alumina samples. In the case of gaseous reactant systems, the higher alumina surface area provides increased surface reaction sites.

Mass transfer limitations were especially prominent in alumina chlorinations when $CO-Cl_2$ or $COCl_2$ were used. Alder (2) fit a Knudsen pore diffusion model to data obtained for the reaction of alumina with gaseous reactants which supports the idea that pore diffusion mass transfer limits the reaction rate. Mass transfer has not been stressed previously, but alumina, having a high surface area (up to 280 M^2/g), is a material likely to be mass transfer limited. No mass transfer effects were mentioned for chlorinations in which admixed solid reductants were used.

Iron oxides

Fruehan and Martonik (17) studied the chlorination of pure iron oxide and an iron oxide ore. The pure iron oxide was 99.9 percent hematite, had a surface area of 0.008 M^2/g, and a density of 4.83 g/cc. The ore was 96.2 percent hematite, 1-2 percent wuestite, and 1-3 percent silica with a surface area of 0.14 M^2/g and a density of 3.56 g/cc. Physical characteristics were found to be very important parameters when determining reaction rates.

Chlorinations were done using a recording semi-microbalance. The total gas flow rate, consisting of a mixture of helium or argon and hydrogen chloride gas or chlorine, was 2 liters (STP) per minute. The temperature range studied was 800 to 1200°C. The reaction rate was influenced by gas composition. When argon was used as the inert part of the feed, the reaction rate was 50 percent slower than when helium was used which indicates that gas diffusion was a limiting condition. The reaction rate of the iron ore was more rapid than that of the pure oxide for temperatures below 1000°C. It was stated that the higher surface area of the ore produced the higher reaction rate.

Particle sizes were also important. For material with diameters of 0.2 centimeters or less, the reaction rates were equal. However, for particle diameters larger than 0.2 centimeters, the rate dropped off rapidly. Microscopic examinations of partially reacted oxide or ore particles showed that there was a hard, unreacted core covered by a fluffy outer layer. This is quite different from the observations of partially reacted alumina (2) where the alumina particles hollowed out.

In another set of experiments (38), hematite, magnetite, and wuestite were chlorinated with pure chlorine; the same materials were also chlorinated in admixture with solid carbon. Physical property data were not reported. Both thermogravimetric (TGA) and batch-boat experiments were run to determine the effects of temperature, chlorine flow rate, feed composition, reaction period, and carbon content.

The oxide reactions were slight at temperatures below 700°C in the absence of carbon and increased little as the temperature was increased. However, conversions were higher at all temperatures as the carbon content of the mixtures was increased. The chlorine feed concentration was not extremely important, but, as the flow rate increased, the reaction rate did increase slightly.

Piskunov, et al. (40) studied the reaction of hematite with hydrogen chloride gas using a small fluidized-bed reactor. The hematite was formed into briquettes, sintered, and then crushed to - 60 + 100 mesh. No solid reductants were used and the temperature was varied from 700 to 950°C. After a chlorination period of 20 minutes, the conversion at 700°C was only 4 weight percent; however, at 950°C, for the same time period, the conversion increased to 36 weight percent. In addition to being a strong function of the temperature, the conversion was also found to be affected by the HCl gas concentration.

These results again indicate the importance of certain reaction parameters. First, the surface area of the iron oxides was important. Chlorination of the more porous iron oxide ore was more rapid than that of the dense reagent-grade oxide. Particle size, one factor in determining surface area, was significant. As the particle size decreased down to 0.2 centimeters diameter, the reaction rate increased. The particle size decrease, in addition to increasing the surface area, also reduces the lengths of the diffusion paths for reactants and products. This serves to reduce pore diffusion effects on reaction rates.

Reaction Mechanisms

The general observations listed along with some more obscure ones, were often explained by proposing reaction mechanisms. The solid reductant role in the chlorination reaction mechanism has received considerable attention. If the solid reductant function was explained, it would be easier to understand why its high surface area and proximity to the primary reactant are important.

Bergholm (6) determined that the distances between carbon and titania particles had to be less than 200 microns for reactions to occur at an appreciable rate. This suggested the presence of an unstable, intermediate compound. Such intermediates as COCl, and Cl atoms were proposed. If the distances between the primary reactant and carbon were too great, the intermediates may not be formed. Milne (34) suggested that in the chlorination of bauxite, the reaction takes place through a $COCl_2$ complex chemisorbed on the alumina surface. No further details were given.

Two Russian abstracts (25, 47) suggested that chlorine adsorbs on the carbon surfaces and dissociates into atoms. The atoms then travel to the metal oxide surface where reaction takes place. The extent of reaction was limited because of loss of surface contact between the metal oxides and carbon. A slightly different explanation was given in another Russian abstract (21). Here, the carbon and metal oxide surfaces served as adsorption surfaces for moles and atoms of chlorine and radicals of chlorine and carbon monoxide. The chlorine displaces oxygen from the metal oxide and the freed oxygen reacts with carbon or carbon monoxide to form carbon monoxide or dioxide. Two other Russian abstracts (28, 30) proposed yet a different mechanism. Instead of adsorbing on the carbon surface, the chlorine adsorbed onto the oxide surfaces. The chlorine adsorption weakened the metal-oxygen bonds and the metal oxide was then easily reduced by carbon. Once the oxide was reduced, it quickly reacted with chlorine to form chlorides. Therefore, the progress of the reaction was said to be limited by the reduction step.

The carbon, besides being a surface for production of reaction intermediates, must react with freed oxygen to shift the equilibrium toward the chloride. In the case of alkaline earth oxides, the chlorine reacted directly with the oxide to produce chlorides and oxygen. The carbon had to react with oxygen to perpetuate the reaction (25). Landsberg (31) speculated that the carbon-oxygen reaction could limit the chlorination rate of clays. This was proposed because the activation energy for the reactions in which carbon was used as the reductant corresponded to that for the burning of carbon with oxygen. Alder (2) drew the same conclusion about the chlorination of pyrolytically carbon coated alumina. Carbon was burned with oxygen to give an activation energy comparable to those obtained for the alumina chlorinations.

Morris and Jensen (37) formulated a reaction rate equation for the chlorination of rutile. Fractional partial pressure exponents were calculated that suggested the rutile surface was covered with a primary reactant product such as $TiOCl_2$ or $TiCl_2$. These intermediates are thought to be stable, and therefore limit the surface area available to the reactants, CO and Cl_2. Other evidence of intermediate metal compounds was presented in a Russian abstract (22). Thermogravimetric, thermographic, and X-ray diffraction analyses indicated that the chlorination of rutile, using CO and Cl_2, proceeded through a $TiOCl_2$ intermediate.

Phosgene was shown to be by far the best secondary reactant for temperatures below 700°C. It is not as effective above 800°C because it dissociates into CO and Cl_2 (2, 6, 31). Improved kinetics was given as the reason for the great efficiency of phosgene below 700°C (6, 31). Both the chlorinator and reductant are present simultaneously at the reaction site. Bergholm (6) suggested that phosgene dissociates into highly reactive components such as Cl atoms and COCl radicals.

Fly Ash Chlorinations

Wijatno (51) chlorinated the nonmagnetic fraction of magnetically separated fly ash. The magnetic separation removed 75 weight percent of the iron oxide originally present in the whole ash giving a nonmagnetic fly ash fraction with the following weight percent composition: 46.9 SiO_2, 18.8 Al_2O_3, 6.6 Fe_2O_3, 5.4 CaO, 1.5 MgO, 1.7 K_2O, 0.4 Na_2O and 2.3 SO_3. The loss on ignition, due mainly to unburnt carbon, was 11.5 weight percent. No surface areas or particle size distributions were given for this material.

Chlorinations were conducted using a horizontal, packed-bed reactor. The nonmagnetic ash was mixed with graphite in the weight ratio of 10:3. One set of experiments was directed toward removing the iron oxide without removing alumina. Since iron oxide has a higher affinity for chlorine than alumina, most of the iron should be separable from the nonmagnetic fly ash by chlorination. Therefore, a low chlorine flow rate was used to see if iron oxides would be preferentially chlorinated. The temperature range tested was 550 to 850°C. The best results, 1.1 weight percent of the alumina removed and 41.4 weight percent of the Fe_2O_3 removed, were obtained for a 1/2-hour chlorination at 550°C. Above 550°C, the alumina was chlorinated too extensively.

In a second set of experiments, ten-gram samples of carbon-fly ash were chlorinated at higher temperatures. The chlorine flow rate was maintained at 44 cc/min, a rate limited by reactor geometry. Higher flow rates caused elutriation of bed material. The chlorine flowed through a horizontal, fixed-bed of the sample mixture. These chlorinations differ from most of the previously discussed research with bauxite, clays, and titania ores. In those experiments, chlorine gas flowed over samples contained in boats, whereas in this research, the chlorine flowed through the bed of sample material. The reaction period was

2 hours and the temperature range was 750-900°C. The highest alumina conversion of 81.4 weight percent was obtained for the 900°C chlorination. As temperature and reaction period increased, the alumina conversion increased, however, the conversion was not a strong function of temperature. At 800°C, for a 2-hour period, the alumina conversion was 70 weight percent. This is not greatly different from the 81.4 percent alumina removed at 900°C.

It was concluded that the chlorination of this coal fly ash was mass transfer limited. Based on the other studies mentioned, mass transfer limitation seems very unlikely. An average particle size of 31 microns diameter was given. No surface area data were presented but even if the particles were very porous, with such small diameters, there should have been no pore diffusion mass transfer limitations. However, mass transfer limitations concerning the chlorine flow could have been important. With such small particles in a packed-bed, channelling patterns could have created a maldistribution of the chlorine flow.

Literature Summary

Having considered the reaction systems, the reaction conditions, and results, several general observations will be listed.

1. The secondary reactants, listed in order of decreasing effectiveness, are: phosgene, pyrolytic carbon-chlorine, carbon monoxide-chlorine, and carbon-chlorine.

2. High primary reactant surface areas enhanced the reaction rates, especially when pyrolytic carbon-chlorine and other gaseous secondary reactants were used.
3. High solid reductant surface areas also enhanced the reaction rates. An example was the use of activated charcoal compared to graphite.
4. Mass transfer limitations were appreciable only at high temperatures when the primary reactant had a high surface area or if it was in a briquetted form.
5. The primary reactant-solid reductant particle separation distances were important. This is evident if the reaction rates for the pyrolytic carbon system are compared to those of systems in which carbon was simply mixed with the primary reactant.
6. High temperatures enhanced the reaction rates. Exceptions were for phosgene and systems where mass transfer limited the reaction rate.

EXPERIMENTAL EQUIPMENT AND PROCEDURE

The experimental phase of the work was conducted in three parts: 1) the acid leaching of nonmagnetic fly ash as a pretreatment to chlorination, 2) the chlorination of leached versus nonleached ash to determine the effects of acid leaching, and 3) the chlorination of leached ash conducted with the exit gases analyzed for chlorine, carbon monoxide, and carbon dioxide.

Table 2 lists the chemical composition of the nonmagnetic fly ash fraction used in all of the experimental work. This material resulted from a magnetic separation of a fly ash obtained from the burning of western Kentucky and southern Illinois coals. This is the same ash used in Wijatno's work (51). The ash was collected by mechanical precipitators from a dry bottom type boiler at the Lakeside Power Plant in Milwaukee, Wisconsin. The magnetic separation process has been described previously by Wijatno (51). Unless otherwise specified, whenever fly ash is mentioned henceforth, it should be assumed that reference is being made to the nonmagnetic fly ash fraction.

Acid Leaching of Fly Ash

There were several reasons for acid leaching fly ash. X-ray analyses of the fly ash particle surfaces indicated that the calcium concentration on the surface of the particles was relatively high compared to the calcium concentration in the ash. It was concluded that calcium at least partially coated the surface and, due to its high affinity for chlorine, would be chlorinated before iron oxides, alumina,

Table 2. Composition of the leached and nonleached nonmagnetic fraction of the midwestern bituminous fly ash used in all experiments

Component	Nonleached weight percent	Leached weight percent
SiO_2	47.85	59.05
Al_2O_3	20.59	24.75
Fe_2O_3	7.02	8.76
CaO	5.45	0.84
TiO_2	0.74	0.88
MgO	0.75	0.80
Na_2O	0.36	0.39
K_2O	1.81	2.24
SO_3	1.90	0.66
L.O.I.[a]	11.06	11.26
L.O.D.[b]	0.59	0.89

[a] L.O.I. is loss on ignition from 110-800°C.

[b] L.O.D. is loss on drying from 22-110°C.

or silica. Calcium chloride is not volatile at the chlorination temperatures used, so it was possible that the calcium chloride was blocking the particle surfaces after a short chlorination period and stopping further reaction. Another reason for leaching the ash is that any non-alumina or titania components that could be removed prior to chlorination would represent a savings in chlorine and also serve to simplify the reaction system.

The leaching experimental set-up and procedure were simple. Variables tested were hydrochloric acid concentration, leaching time, and temperature. Fifty ml of acid solution were put in a beaker and brought to the desired temperature. Next, about 5 gm of fly ash were mixed into the acid solution and the suspension stirred throughout the leaching period. The insoluble ash was then filtered out and washed with water. The filtrate was diluted to 250 ml and analyzed for silicon, iron, aluminum, titanium, magnesium, and calcium. Several analytical procedures were employed. In-lab analytical procedures included a CDTA titration (41) for iron and aluminum, an oxalic acid gravimetric procedure for calcium (27), and a gravimetric method for silicon, iron, and aluminum (50). The titration and oxalic acid methods gave reproducible and accurate results while the gravimetric method results were very erratic and nonreproducible. Since there was not an accurate in-lab procedure developed for silicon and titanium determinations, the samples were sent to Analytical Chemistry Group II in the Ames Laboratory where the inductively coupled plasma-atomic emission unit was used to make all of the determinations. These data are listed in Table 3 and plotted in Figures 1, 2, 3, and 4. The calcium oxide and silica results were

Table 3. The amount and weight percent of metal oxides removed as a function of leaching temperature and time and acid strength

Temp. °C	Time min.	HCl conc. M	Metal oxide					
			Al_2O_3 Gms.[a] Wt. %[b]	CaO Gms. Wt. %	Fe_2O_3 Gms. Wt. %	MgO Gms. Wt. %	SiO_2 Gms. Wt. %	TiO_2 Gms. Wt. %
20.0	10	1.0	0.2026	4.8621	0.2590	0.0971	0.5734	0.1896
			0.94	88.4	5.16	30.4	1.18	15.7
95.0	10	1.0	0.6945	5.0936	0.5169	0.1351	1.0304	0.6793
			3.21	92.6	10.3	42.2	2.13	56.1
22.0	10	3.0	0.2328	4.8512	0.3024	0.1001	0.6008	0.2471
			1.08	88.2	6.02	31.3	1.24	20.4
95.0	10	3.0	0.8829	5.0304	0.9442	0.1490	0.7988	0.7744
			4.08	91.5	18.81	46.6	1.65	64.0
22.5	30	1.0	0.2164	4.8846	0.2746	0.0987	0.6066	0.2186
			1.00	88.8	5.47	30.8	1.25	18.1
95.0	30	1.0	0.9039	5.0499	0.6106	0.1482	0.9992	0.7947
			4.18	91.8	12.2	46.3	2.07	65.7
23.0	30	3.0	0.2626	4.7528	0.3215	0.1008	0.6255	0.2865
			1.21	86.4	6.40	31.5	1.29	23.7
95.0	30	3.0	0.9589	5.0527	1.1930	0.1554	0.6952	0.8221
			4.43	91.9	23.8	48.6	1.44	67.9
95.0	10	6.0	1.0060	5.0318	2.4003	0.1564	0.5772	0.8545
			4.6	91.5	47.8	48.9	1.19	70.6
101.0	30	6.0	1.4801	5.0588	3.2378	0.1857	0.5016	1.1810
			6.84	92.0	64.5	58.0	1.04	97.6
22.0	10	6.0	0.2581	4.8947	0.3542	0.1004	0.5481	0.2805
			1.19	89.0	7.06	31.4	1.13	23.2
22.0	30	6.0	0.2991	4.9004	0.3761	0.1038	0.5541	0.3201
			1.38	89.1	7.49	32.4	1.15	26.4

[a] Gms. are the grams of an oxide removed from a 100-gram sample of nonmagnetic fly ash.

[b] Wt. % is the weight percent of an oxide removed from a 100-gram sample of nonmagnetic fly ash.

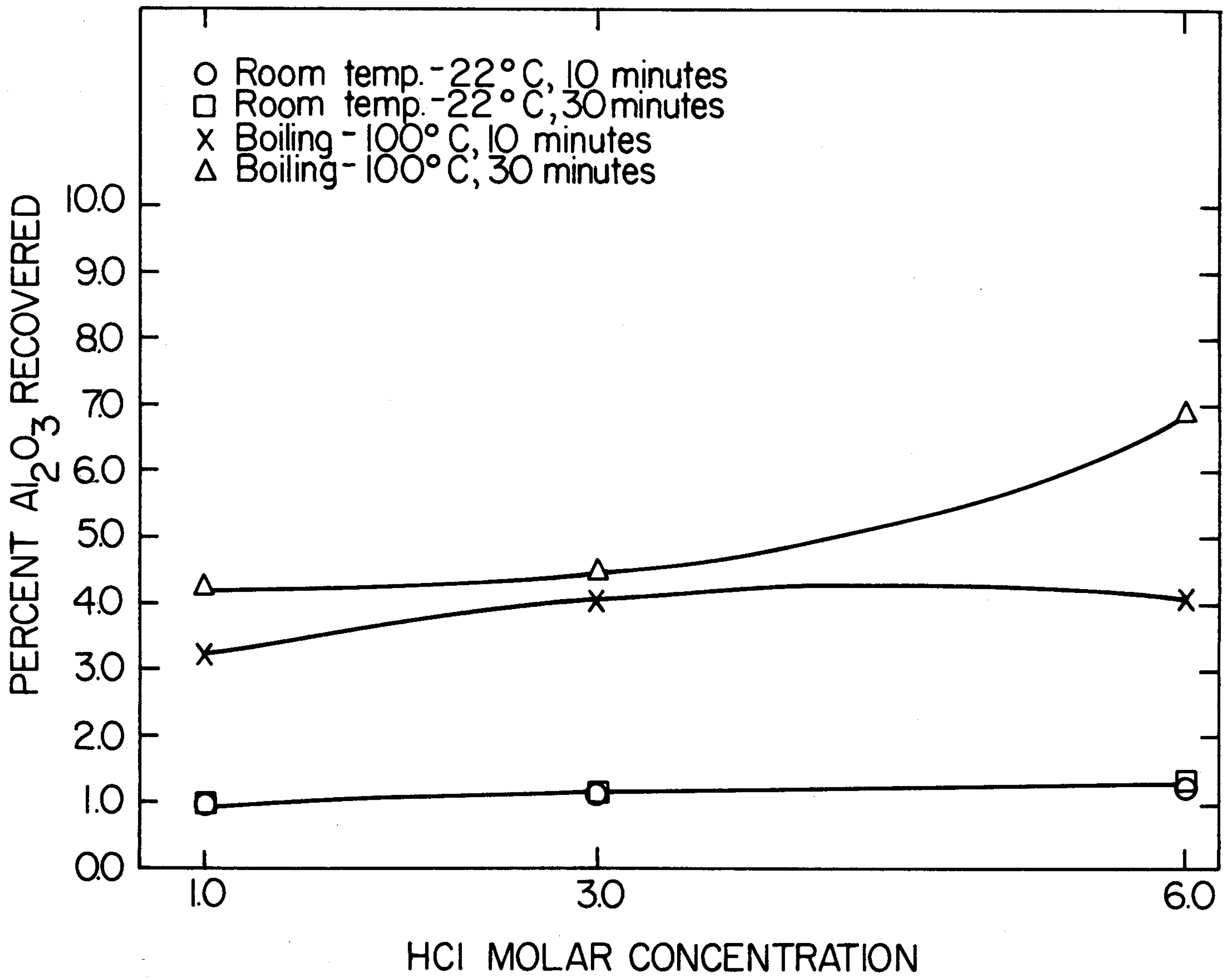

Figure 1. The effect of HCl molar concentration on alumina recovered for different reaction temperatures and times from the midwestern bituminous, nonmagnetic fly ash fraction used in all experiments

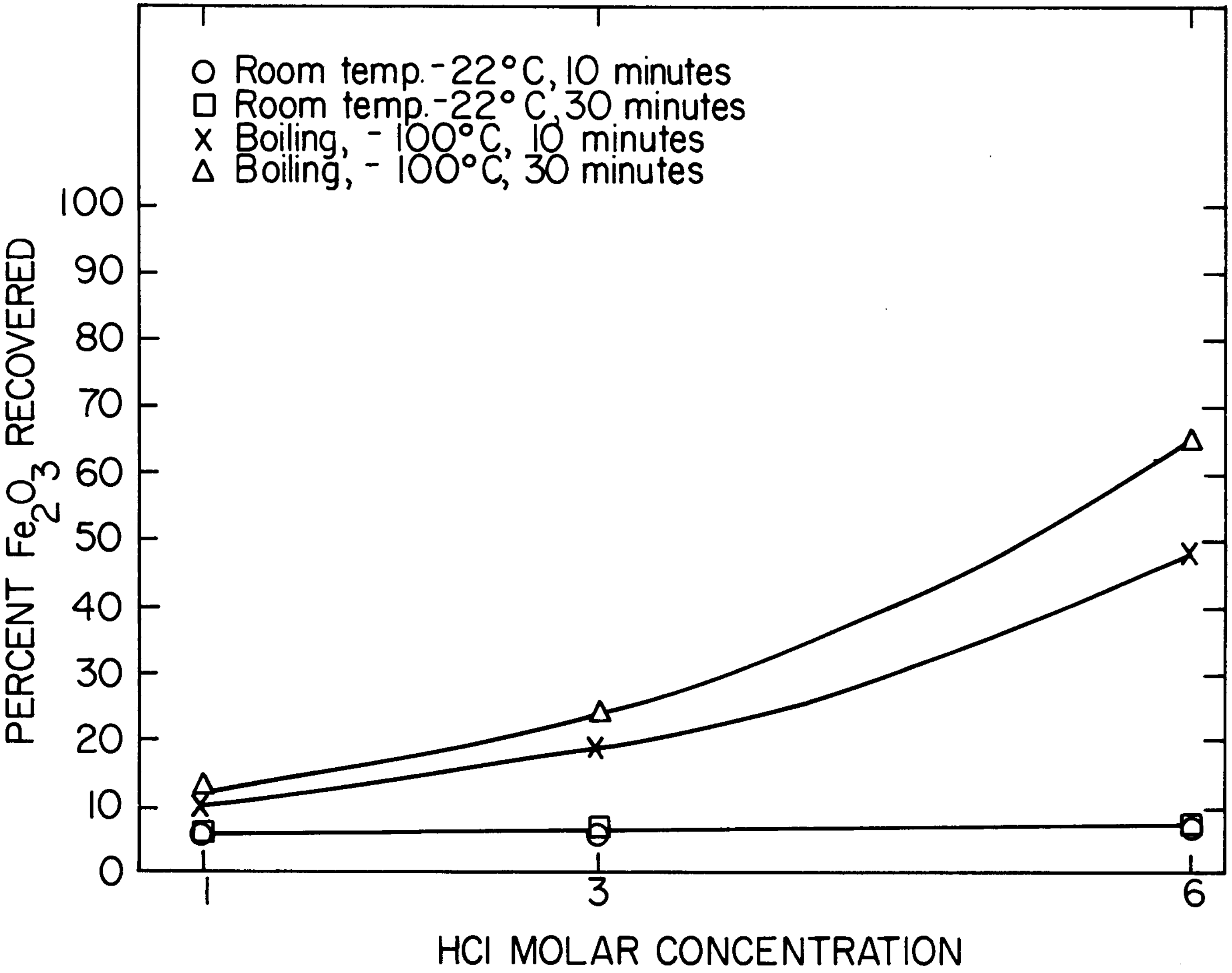

Figure 2. The effect of HCl molar concentration on iron oxide recovered for different reaction temperatures and times

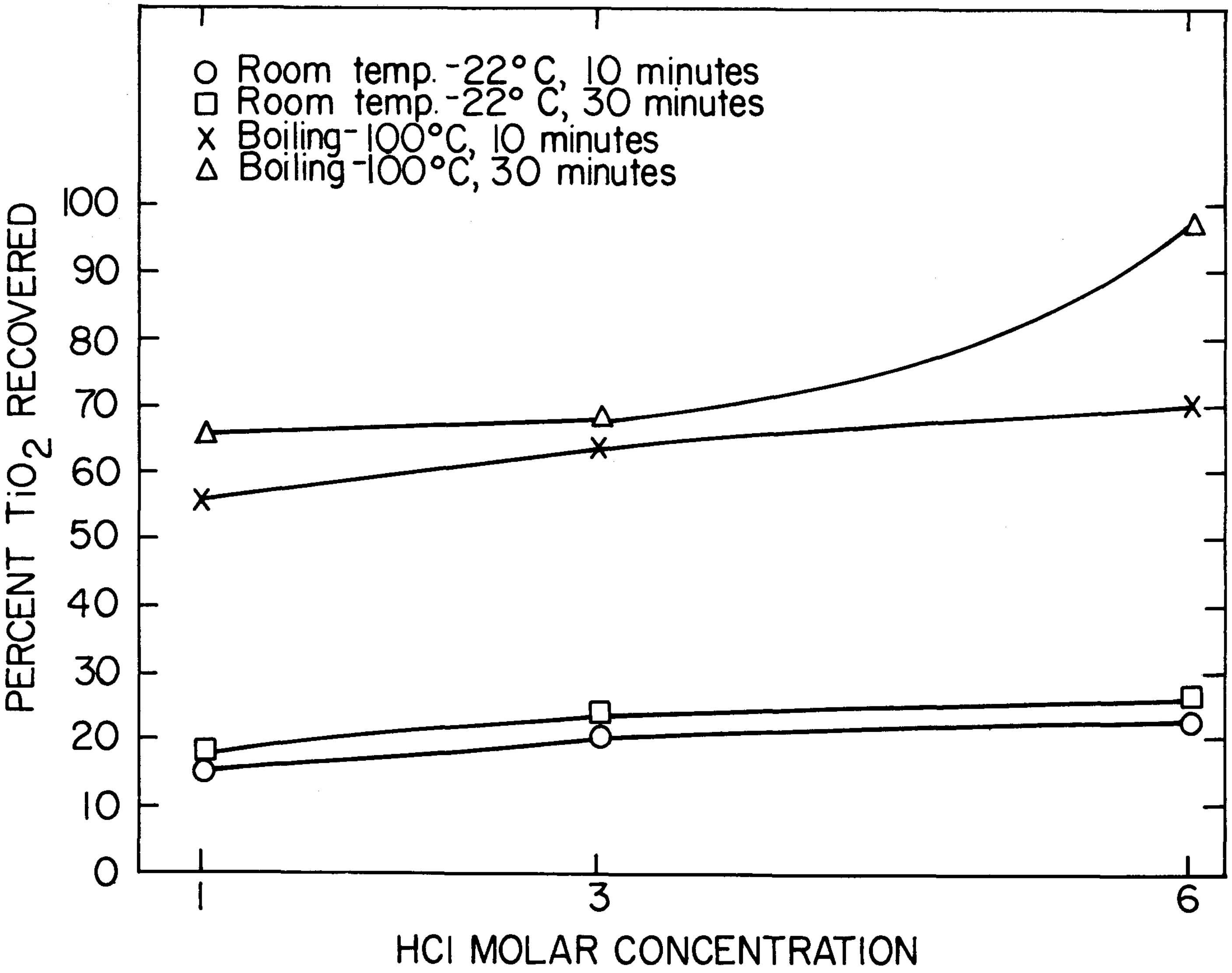

Figure 3. The effect of HCl molar concentration on titania recovered for different reaction temperatures and times

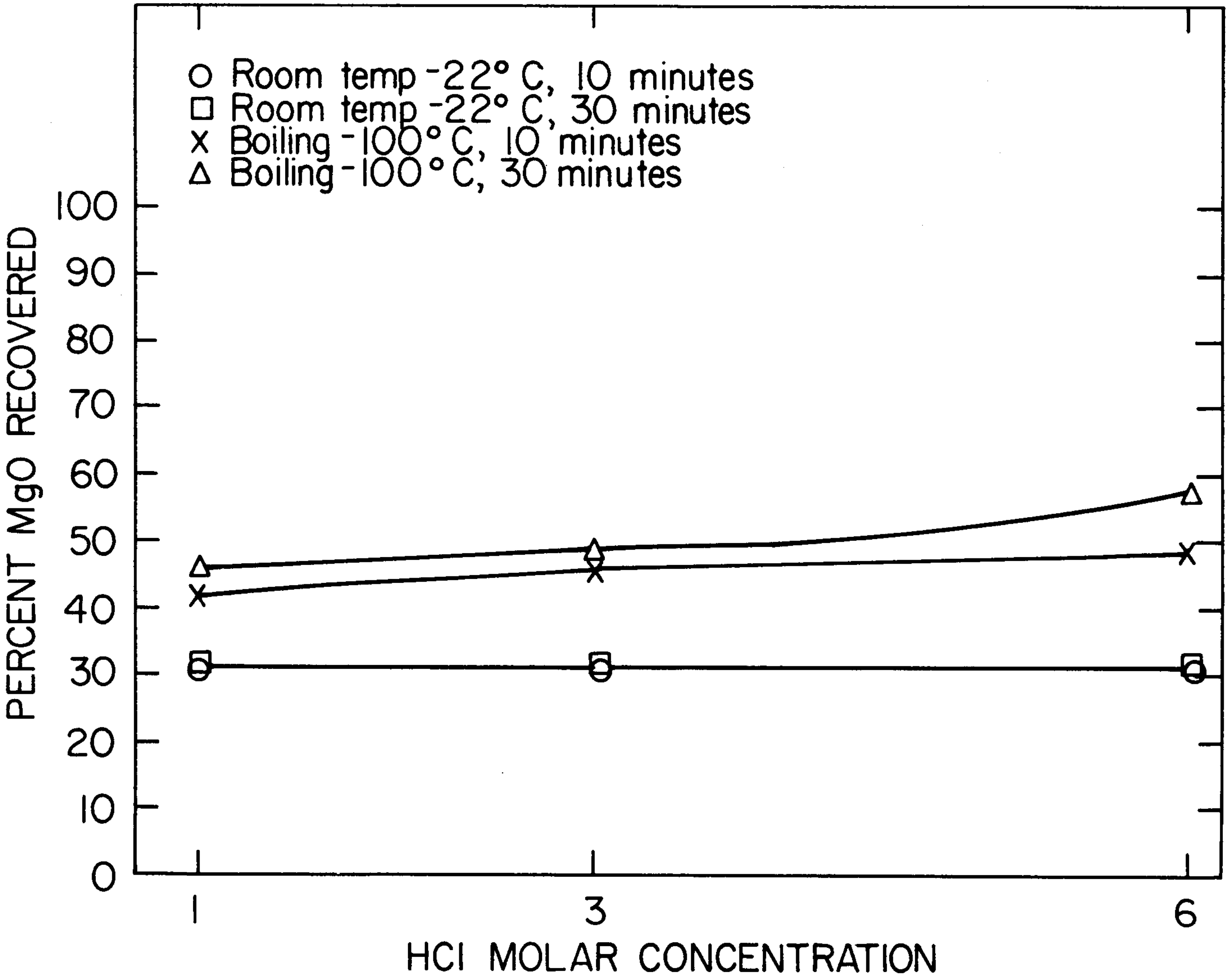

Figure 4. The effect of HCl molar concentration on magnesium oxide recovered for different reaction temperatures and times

not plotted because the amounts removed were nearly constant for all conditions tested.

The results indicate that the removal of aluminum, iron, titanium, and magnesium depended on the acid strength only when the leachings were conducted at 100°C. Also, time effects are most pronounced for leachings at 100°C using 6 molar HCl solution; the percentages removed at 30 minutes are considerably greater than those for 10-minute leachings. This would indicate some rate limitation for the reaction. The most severe leaching conditions, 6 molar HCl at 100°C for 30 minutes, were very effective in removing iron, calcium, titanium, and magnesium. As was mentioned, the major objective of the leachings was to remove nonalumina materials. However, calculations show that the alumina content of the leached ash as compared to the nonleached ash is only increased by 2 weight percent. This amount of alumina enrichment would not justify such a severe leaching treatment.

It was then decided that a less severe set of leaching conditions, 22°C, 1 molar HCl, and 30 minutes, would remove most of the calcium while taking very little of the aluminum. The filtrates were not analyzed for potassium but the data in Table 2 indicate that most of the potassium stayed in the ash. Sodium and magnesium concentrations are negligible and can be ignored.

Chlorination of Leached and Nonleached Fly Ash

The next experimental section started with leaching a large batch of nonmagnetic fly ash with 1 molar HCl for 30 minutes at 22°C. The leached ash was analyzed and the results are listed in Table 2. Chlorinations of leached versus nonleached ash were then conducted using an experimental set-up closely resembling that employed by Wijatno (51). A Matheson chlorine gas regulator and a Brooks rotameter were used to control the flow of high-purity chlorine (99.5%, Matheson) to the reactor. A calcium chloride trap was put in line between the regulator and rotameter to dry the chlorine. The reactor was made of 25-millimeter Vycor tubing and had a ball joint at the entrance and a large ground glass joint at the exit. The reactor was heated by an electric resistance furnace. The large exit ground glass joint was not heated. As the reaction products exited through the ground glass joint, the cross-sectional area expanded, slowing the flow velocity and causing a large amount of the higher melting-point products to condense inside the joint. The rest of the products were condensed in a cold-finger trap at liquid nitrogen temperatures. The reactor temperature was monitored by an alumel-chromel thermocouple taped to the side of the reactor at the middle of the reaction zone. A Sargent recorder was used to monitor the thermocouple output.

The following procedure was used. About 100 gm of 10:3 weight ratio leached or nonleached fly ash to graphite were mixed in a ball mill for 1 hour. A 10-gm sample was then dried in a porcelain crucible at 300°C for 1 hour, cooled in a desiccator, and reweighed. The carbon-ash mixture was poured into the reactor along with 0.5-cm quartz chips, added to increase the porosity of the bed. The loaded reactor was then put in the furnace and purged with a slow flow of argon until the desired operating temperature was reached. The cold finger dewar was filled with liquid nitrogen and the chlorine flow was started and maintained at the desired rate until the chlorination period expired. The chlorine was then turned off, but the furnace temperature was maintained for 15 minutes while the reactor was purged with argon. The furnace was next turned off and opened for rapid cooling so the reactor could be removed and the reaction products rinsed out into a large beaker. The chlorination product solution was evaporated to dryness and the residue was scraped out of the beaker and stored until analyzed. The remaining, unreacted residue was tapped out of the reactor, separated from the chips, dried for 1 hour, cooled in a desiccator, and weighed to permit calculation of the weight loss for the reaction and then analyzed for component losses. A component mass balance was made between the products collected and the residue losses. The agreement was usually within ± 5 weight percent.

Fly Ash Chlorination with Product Gas Analysis

After reviewing the data from the first set of chlorinations, it was decided that more detailed information was needed in order to understand or explain what was happening during the chlorination. It was decided to analyze the noncondensible product gases and excess chlorine using gas chromatography. The reactor system shown in Figure 5 was then designed and assembled.

<u>Gas chromatography experimental system</u>

A 7400 series rotameter assembly from Matheson was used to monitor the flow of CO, CO_2, and Cl_2 through the reactor system. The rotameter

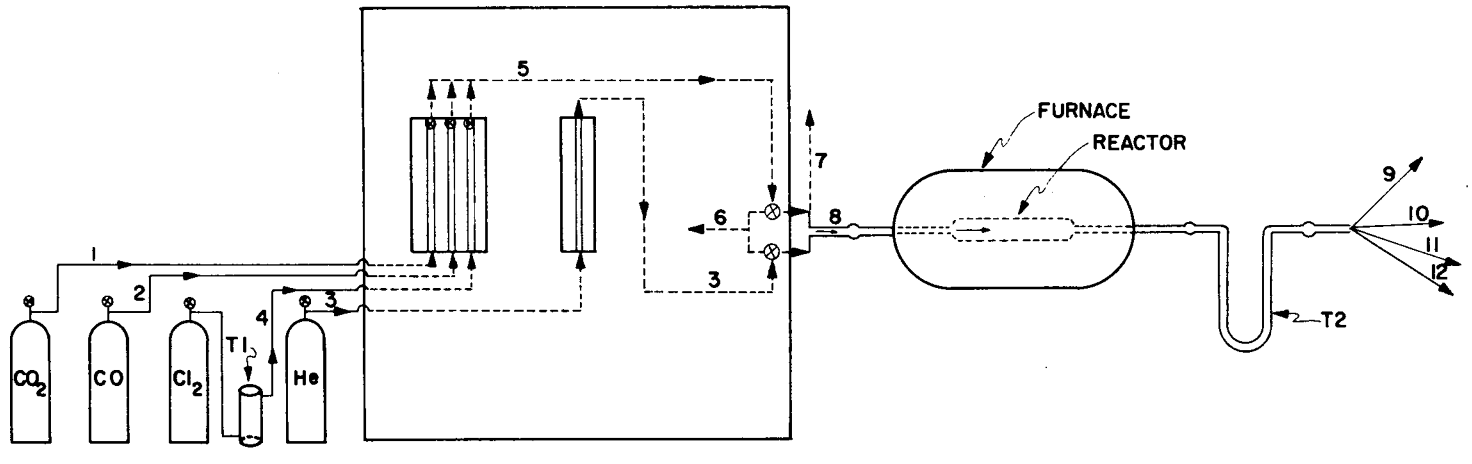

1. Carbon dioxide supply stream used to calibrate GC.
2. Carbon monoxide supply stream used to calibrate GC.
3. Helium supply stream used for reactor purge.
4. Chlorine feed stream to reactor and to GC for calibration.
5. Connecting line between rotameter bank and reactor.
6. Vent line to allow for purging gas lines up to reactor.
7. Manometer line used with 9 to measure pressure drop across reactor.
8. Line through reactor.
9. Manometer line used with 7 to measure pressure drop across reactor.
10. Line to manometer used to measure net pressure on system.
11. Line connected to GC sampling valve.
12. Vent line to allow escape of excess gas not going into GC.

T1. Calcium chloride trap used to dry chlorine.
T2. Magnesium perchlorate trap used to dry reactor exit stream.

Figure 5. Schematic diagram of chlorination equipment

assembly consisted of three separate flow tubes and a mixing tube. Helium gas was used as the reactor purge gas because it was the same as the gas chromatograph carrier gas. The helium flow was controlled by a rotameter from LAB Crest Division, Fisher and Porter Co. The reactor was nearly the same size as the one used previously and, during the chlorinations, the reactor was again positioned horizontally. At the reactor exit, there were four branchlines. Two were used as manometer leads, another was connected to a reactor vent valve, and the last was connected to the gas chromatograph (GC) sampling valve. One manometer measured the pressure drop across the bed and the other measured the net pressure of the reactor system as compared to the ambient pressure. A net system pressure of 0.1 atmospheres was required to force product gases into the sampling loop. A magnesium perchlorate trap was placed in line between the reactor and the GC to absorb any water in the product stream. Efforts were made to minimize dead space in the reactor system so residence times would be short and gas mixing effects would not greatly affect the GC results.

Gas chromatograph

A Model 720 dual column gas chromatograph manufactured by Hewlett Packard and F&M Scientific Division was employed for the gas analyses. The chromatograms were recorded by an Electronik 15 Chromatography Recorder. The GC used thermal conductivity cells for detection. A Carle Instruments, Inc. Model 2014 gas sampling valve delivered 2.5 ml of sample gas to the GC. The same GC conditions were used for all analyses. The Wheatstone bridge current was 150 mA, the detector block temperature was maintained at 60°C, the separation column was submerged in ice water contained in a dewar, and the carrier gas flow was 23 cc helium per minute. The separation column consisted of a 10-foot long, one-eight-inch diameter teflon tube packed with 15 gm of 60/80 mesh Carbopack B that was coated with 10 weight percent phosphoric acid. Carbopack B is a graphitized carbon black with a surface area of about 100 M^2/g (12). The column gave 4-5 minute separations of CO, CO_2, and Cl_2. Since one column gave the desired separations, the second column consisted of a blank, one-fourth inch diameter stainless steel tube. The dual column chromatograph was operated by using one-half of the detector as the reference for the other half. Thus, the helium gas flowing through the blank column served as the reference.

Operating procedure for the gas chromatography system

The same sample preparation, reactor loading, and heat-up procedures mentioned for the earlier chlorinations were followed. A more sensitive temperature recorder manufactured by Leeds & Northrup was used; the reactor temperature could be controlled to within ± 2°C. During heat-up, a tube bypassing the reactor and connected between the GC sampling valve and the 4-tube rotameter bank was used to deliver CO, CO_2, and Cl_2 mixtures of known proportions to the GC so calibration curves could be recorded. When the reactor reached the desired run temperature, the chlorine was turned on and the gas analyses were started. At the end of the chlorination period, the chlorine was turned off and the reactor was purged with helium until no more product peaks appeared on the GC output. The bypass tube was again connected and another set of CO, CO_2, and Cl_2 standard curves were recorded to check if the GC sensitivities had changed during the run.

The gas sampling valve and reactor vent streams were combined and flowed through a bubble-flow meter. The GC data, when combined with the flow rates measured during the run, gave flows of CO, CO_2, and Cl_2 exiting the reactor as a function of time. The solid residue was analyzed for component losses. No chloride products were collected because the silicon tetrachloride gas is difficult to trap and usually escaped. The agreement between product component amounts collected in the liquid N_2 trap and residue losses **in** the earlier runs was excellent, and therefore, analysis of the residue alone was considered to be sufficient.

In the leached versus nonleached chlorinations, the only experimental parameters varied were temperature and reaction period. The chlorine flow was held constant at about 25 cc per minute and the fly ash to graphite ratio was always 10:3. The temperatures used were 750, 800, 850, and 900°C and the reaction periods were 1/2, 1, and 2 hours. Therefore, to test all possible combinations of time and temperature for a comparison between leached and nonleached ash, 24 chlorinations were completed. Only a few duplicate chlorinations were done. When the next system, employing the GC, was used for chlorinations, only 2-hour chlorinations were conducted for the temperatures listed and only leached ash was chlorinated. Duplicate runs were made at each temperature making a total of 8 runs. Again, the fly ash to graphite weight ratio was 10:3 but the chlorine flow rate was raised to 30 cc per minute. These runs then gave the CO, CO_2, and Cl_2 flow rates as a function of time for leached ash over a 2-hour period. The elemental composition of the ash was also known for four points over the same 2-hour period as a result of the first set of chlorinations.

Analytical Methods

Accurate, fast, and comprehensive analytical methods were felt to be very important to this research. Several elements of interest needed to be analyzed in a large number of samples. During the search to find an analytical tool that would give the desired results, several methods were tried. The methods investigated are listed with references for the metals they were used to determine. A short discussion of the merits and/or shortcomings of each method follows the list.

Method	Elements determined
Gravimetric (50)	Silicon, aluminum, iron, and calcium
CDTA titration (41)	Iron and aluminum
ASTM colorimetric (44)	Iron, aluminum, titanium, and silicon
Atomic absorption spectrophotometry (3)	Iron, aluminum, titanium, and silicon

The gravimetric method was not used extensively because accurate results were obtained for calcium only when standard solutions were analyzed. One particular step required the separation of aluminum hydroxide from the solution by precipitation of only aluminum hydroxide. When this precipitate was filtered and ashed, the residue usually had a red tint indicating the presence of iron oxides. The aluminum hydroxide apparently pulled some iron out of solution also.

The CDTA titration gave excellent results when tested on standard solutions of iron and aluminum, however, its applicability was limited to iron and aluminum determinations. There was also a potential problem with the iron analysis. In the method, aluminum was masked by adding ammonium fluoride to the sample solution and the iron was complexed by adding excess CDTA. The extra CDTA, not complexed with iron, was then back-titrated with lead nitrate solution. However, when the excess CDTA was added, the titanium in the solution was also complexed and therefore appeared as iron. For the samples analyzed in this study, the titanium was a minor problem because the concentration was negligible compared to the iron or aluminum.

A colorimetric analyses scheme was employed next. Accurate results were obtained for iron, aluminum, and titanium, however, silicon results were usually low. The silicon inaccuracies cannot be explained without first mentioning steps prior to the colorimetric analyses. Solid residues were fused into solution using a lithium metaborate based procedure (7, 45). This method was used because lithium metaborate fusions are much faster and less dangerous than the liquid sodium hydroxide fusions required by the ASTM Method (44). The colorimetric scheme specified the sodium hydroxide fusion, therefore, the silicon problem could be the result of solution matrix changes due to the lithium metaborate or to a lack of activation of the silicon by the metaborate. If some of the silicon was not in a form that was reactive with the coloring agents, then low values would be obtained. Other disadvantages of the colorimetric method were the large sample dilutions and the many reagent additions required, which made the method subject to error and very time consuming.

Atomic absorption spectrophotometry (AAS) has been found to be the most reliable and convenient method of those tested and is now being used for all in-laboratory analyses. The solid samples are fused and then analyzed with a Model 373 Perkin-Elmer AAS unit. Individual elemental sensitivities and machine standard operating conditions are specified in a methods book which accompanied the unit (3). Iron, aluminum, titanium, silicon, calcium, and magnesium are analyzed quickly and accurately by this method.

RESULTS AND DISCUSSION

Effects of Acid Leaching Fly Ash Prior to Chlorination

The purpose of the first series of experiments was to determine the effects of acid leaching nonmagnetic fly ash prior to chlorination. The solid residues remaining after the chlorinations were analyzed for iron, titanium, aluminum, and silicon losses. These data are listed in Table 4 as moles and mole percents of an oxide removed. In addition, the moles of titania, alumina, silica, and iron oxide removed were summed and are listed as total moles oxide removed. The data are listed as moles because the materials react as moles and the mole percents make comparisons for different operating conditions convenient.

Figures 6 and 7 are plots of total moles oxide removed versus reaction time and temperature, respectively. A chlorine flow rate of 0.0010 g-moles per minute was used. This was a very low flow rate considering the initial high reactivity of fly ash and that 10.0 grams was chlorinated. There was usually complete chlorine conversion during the first 15 minutes of the chlorination. In Figure 6 there is a general tendency for the nonleached ash data points to lie below the leached ash points. The points at one-half and one hour are clustered closely together, however, at two hours, there is considerable scatter between the leached and nonleached data points. Since the chlorine conversion was usually quite high during the first hour, nearly the same number of moles were converted for leached and nonleached ash at all temperatures; however, after the first hour, chlorine was in excess, allowing for other reaction parameters, possibly induced by leaching the ash, to

Table 4. Moles x 10^3 and mole percents of oxides removed from leached and nonleached fly ash samples as a function of chlorination time and temperature

		Metal oxide									
		Fe_2O_3		Al_2O_3		SiO_2		TiO_2			
Time hours	Temp. °C	Moles[a] Mole %	Moles[b] Mole %	Moles[a] Mole %	Moles[b] Mole %	Moles[a] Mole %	Moles[b] Mole %	Moles[a] Mole %	Moles[b] Mole %	Total[a] moles	Total[b] moles
0.5	750	1.889	1.507	1.672	2.306	4.351	2.851	0.217	0.169	8.129	6.833
		50.40	44.82	10.11	14.92	6.48	4.68	28.64	23.87		
0.5	800	1.829	1.165	3.275	1.922	4.371	3.219	0.200	0.244	9.675	6.550
		48.86	34.05	19.77	12.22	6.52	5.19	26.42	33.91		
0.5	850	1.758	0.952	3.417	2.156	4.305	2.506	0.241	0.261	9.721	5.875
		46.83	28.00	20.61	13.80	6.41	4.07	31.88	36.57		
0.5	900	1.853	1.024	3.366	1.718	2.292	0.939	0.227	0.259	7.738	3.940
		49.24	30.25	20.21	11.04	3.40	1.53	29.89	36.41		
1.0	750	1.761	2.422	1.465	5.242	–	7.108	0.088	0.237	3.314	15.009
		47.39	71.38	8.91	33.61	–	11.56	11.67	33.27		
1.0	800	2.033	1.863	4.782	6.798	8.226	6.890	0.256	0.327	15.297	15.878
		54.06	55.45	28.74	44.03	12.21	11.32	33.73	46.36		
1.0	850	2.430	2.451	6.934	7.408	8.988	6.775	0.314	0.373	18.666	17.007
		65.47	72.96	42.22	47.99	13.52	11.13	41.97	52.84		
1.0	900	2.631	2.921	6.843	7.411	7.307	7.838	0.292	0.328	17.073	18.498
		70.82	87.45	41.62	48.25	10.98	12.94	38.97	46.73		

---

[a] Moles and mole percent oxides removed from leached fly ash samples.

[b] Moles and mole percent oxides removed from nonleached fly ash samples.

Table 4. Continued

Time hours	Temp. °C	Metal oxide								Total[a] moles	Total[b] moles
		Fe_2O_3		Al_2O_3		SiO_2		TiO_2			
		Moles[a] Mole %	Moles[b] Mole %	Moles[a] Mole %	Moles[b] Mole %	Moles[a] Mole %	Moles[b] Mole %	Moles[a] Mole %	Moles[b] Mole %		
2.0	750	3.074	2.641	9.661	6.928	18.495	4.954	0.519	–	31.754	14.523
		83.10	82.89	58.92	47.80	27.86	8.27	69.41	–		
2.0	800	3.032	2.899	10.955	9.238	21.636	16.827	0.480	0.423	36.103	29.387
		80.75	85.22	65.93	59.10	32.16	27.30	63.31	59.12		
2.0	850	3.109	3.169	11.144	11.096	23.262	18.619	0.465	0.546	37.98	33.430
		83.44	93.50	67.59	71.30	34.85	30.30	61.87	76.40		
2.0	900	3.393	2.997	12.676	11.431	24.269	20.323	0.571	0.527	40.909	35.278
		90.37	88.16	76.30	73.18	36.08	32.99	75.28	73.76		

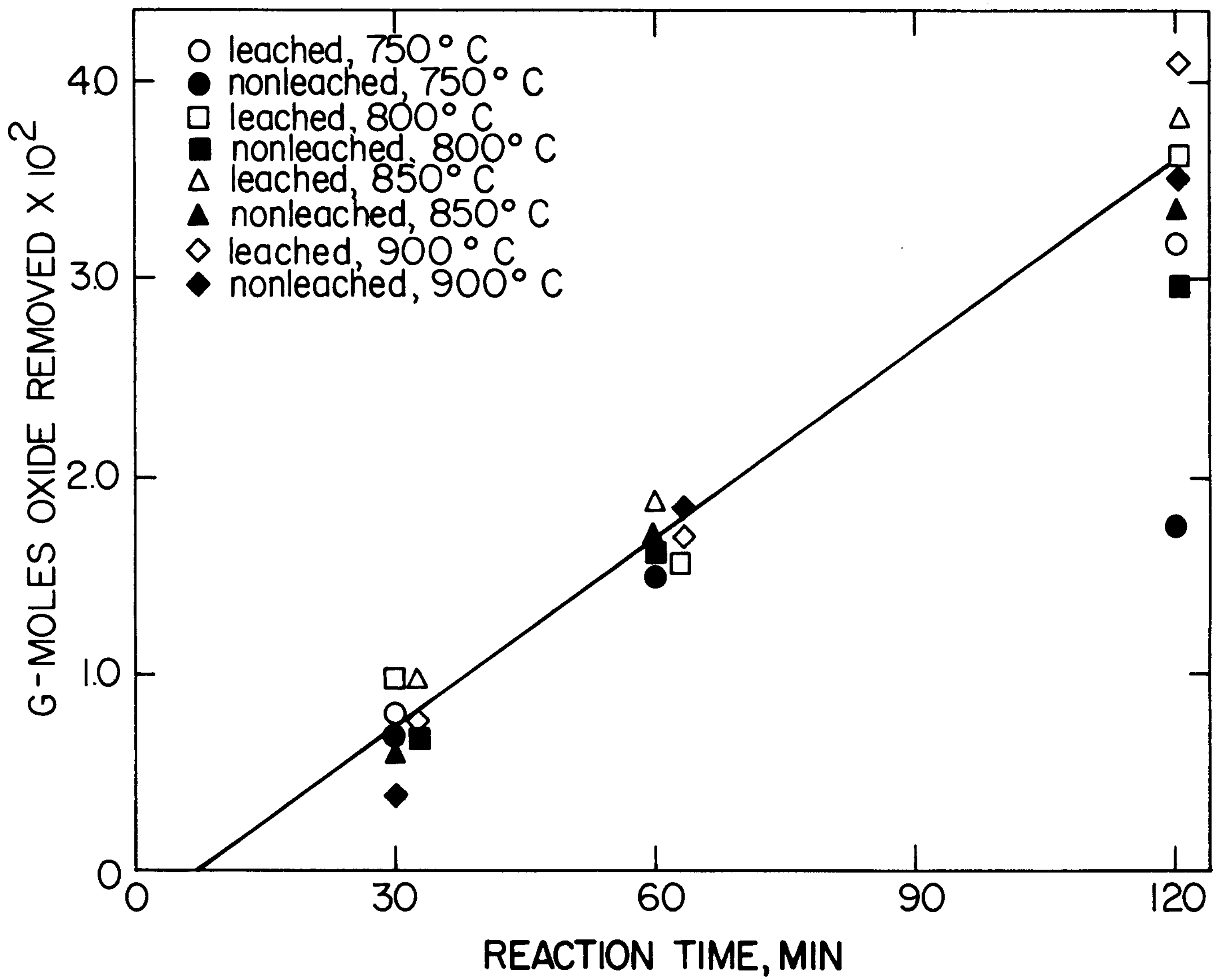

Figure 6. The effect of reaction time on the total g-moles oxide removed at different temperatures for leached and nonleached ash samples. Chlorine feed rate = 0.0010 g-moles/ min

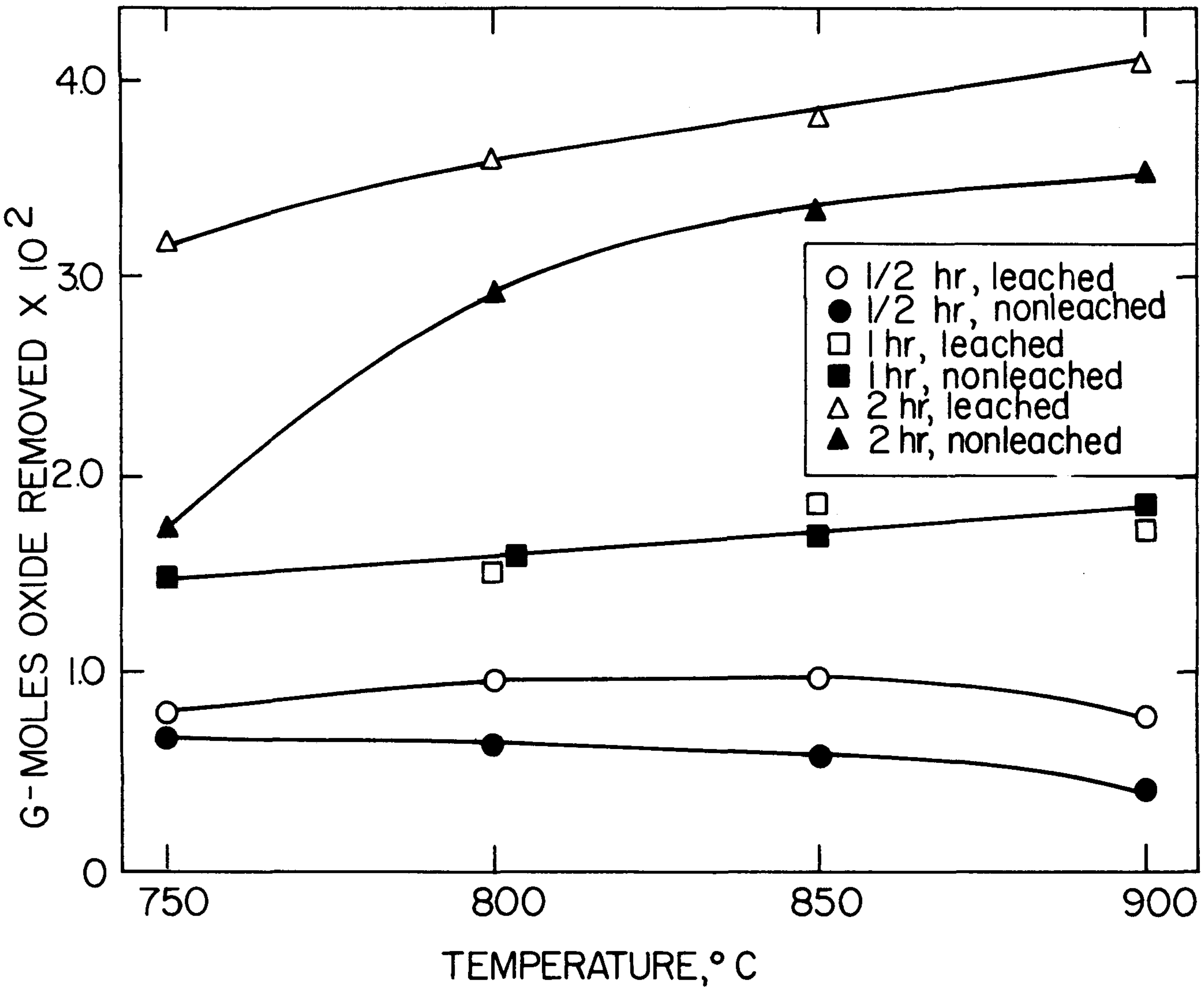

Figure 7. The effect of temperature on the total g-moles oxide removed at different reaction times for leached and nonleached fly ash samples. Chlorine feed rate = 0.0010 g-moles/min

influence the reaction.

In Figure 7, the nonleached points are again lower than the leached ash points, especially for the one-half- and two-hour chlorinations. The gap at one-half hour is due mainly to the calcium oxide present in the nonleached ash. At the chlorine feed rate of 0.0010 g-moles per minute, it would take 7.5 minutes to chlorinate the calcium oxide present in a 10.0-gram nonleached ash sample. Thermodynamically, the calcium oxide is much more reactive with chlorine than iron, aluminum, titanium, or silicon oxides, the compounds represented by the data points. Experiments were done to verify that calcium oxide is reacted at the beginning of the chlorination. Ash chlorinated for one-half hour was leached with water and the filtrate was analyzed to determine that about 90 percent of the calcium oxide was converted to water soluble calcium chloride within the first one-half hour. Therefore, since the calcium oxide is chlorinated first, less chlorine is available to the materials in nonleached ash that are represented by the data points in Figures 6 and 7.

Figure 8 is a plot of moles alumina removed versus temperature for both leached and nonleached ash. There is not a large difference between the moles alumina removed for the two ashes. The leached points are from both sets of chlorination experiments. In the second set of experiments (in which the gas chromatograph was used for analyses) a 1.3 times greater chlorine flow rate was used, but the amounts of alumina removed are comparable. Since more chlorine was available, more alumina should have been removed. The alumina conversion appears to be limited to about 80 percent.

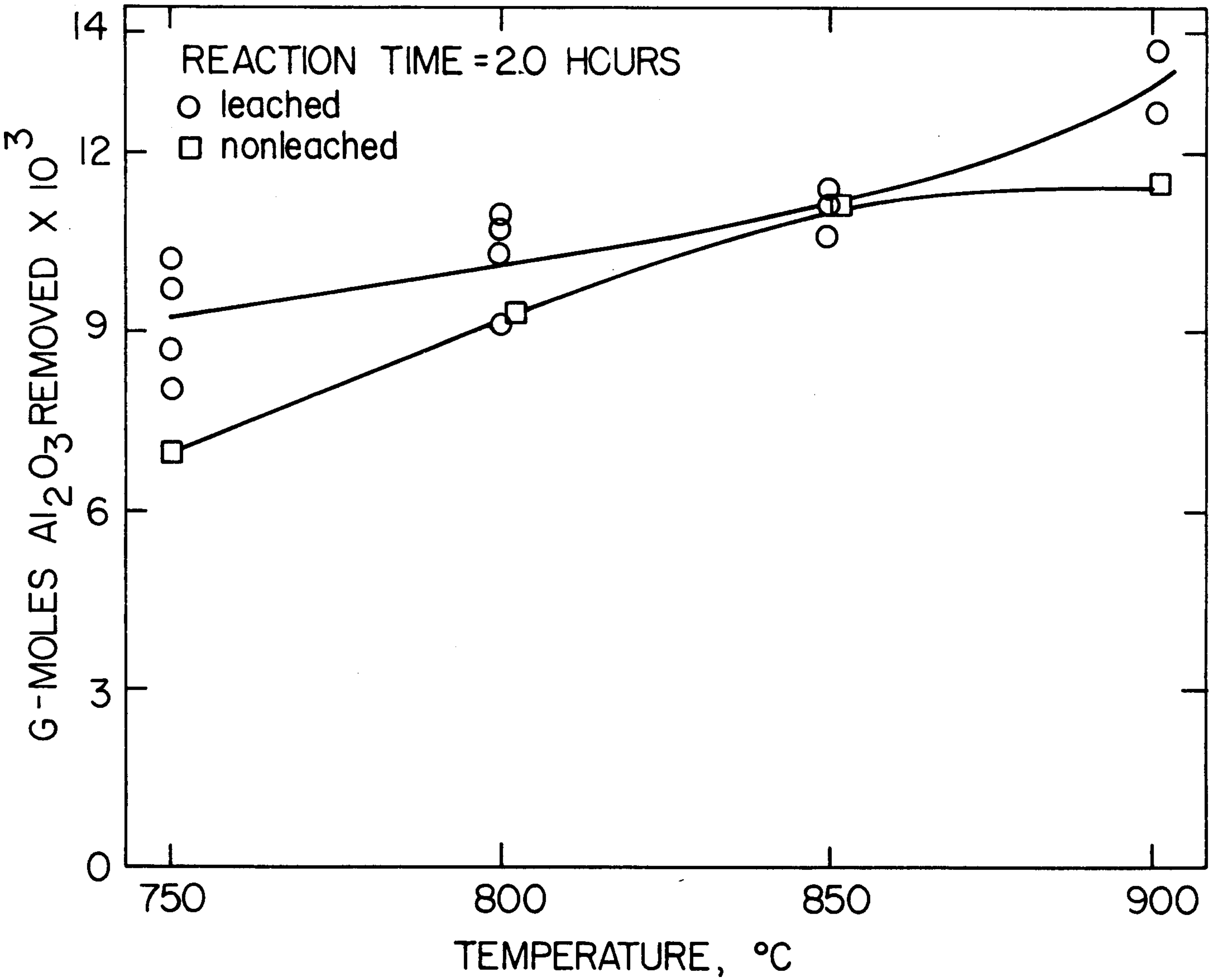

Figure 8. The effect of temperature on the g-moles alumina removed for leached and nonleached fly ash samples. Chlorine feed rate = 0.0010 g-moles/min

The extra chlorine had a more dramatic effect on silica removal. Figure 9 is a graph of moles silica removed versus temperature for two-hour chlorinations. Only leached and nonleached data from the first set of experiments are plotted. The moles silica removed for the gas chromatography (GC) chlorinations are listed in Table 5. The moles silica converted are much higher for the GC chlorinations than those from the first set of experiments listed in Table 4. Evidently the alumina reaction rate slows when conversion reaches about 80 percent and only silica then reacts. This seems logical since silica is the principal compound present by the time the alumina conversion reaches 80 percent.

Due to the low flow rate of chlorine employed, determinations can be made as to whether certain components are preferentially chlorinated. Experimentally, it was determined that calcium oxide reacts first. The data in Table 4 indicate that iron oxide is also preferentially chlorinated ahead of alumina and silica to the extent that iron oxide reacts at a higher rate. However, as can be seen in Table 4, when the iron oxide conversion reaches about 90 percent, the alumina and silica conversions are also high. The mole percents silica and alumina converted depend largely on the reaction period. At one hour, for both leached and nonleached ash, the alumina mole percent conversion is roughly four times greater for alumina as compared to silica. At two hours, the nonleached ash shows an advantage over the leached ash in terms of mole percents alumina and silica converted. The alumina-silica mole percent conversion ratio for the nonleached

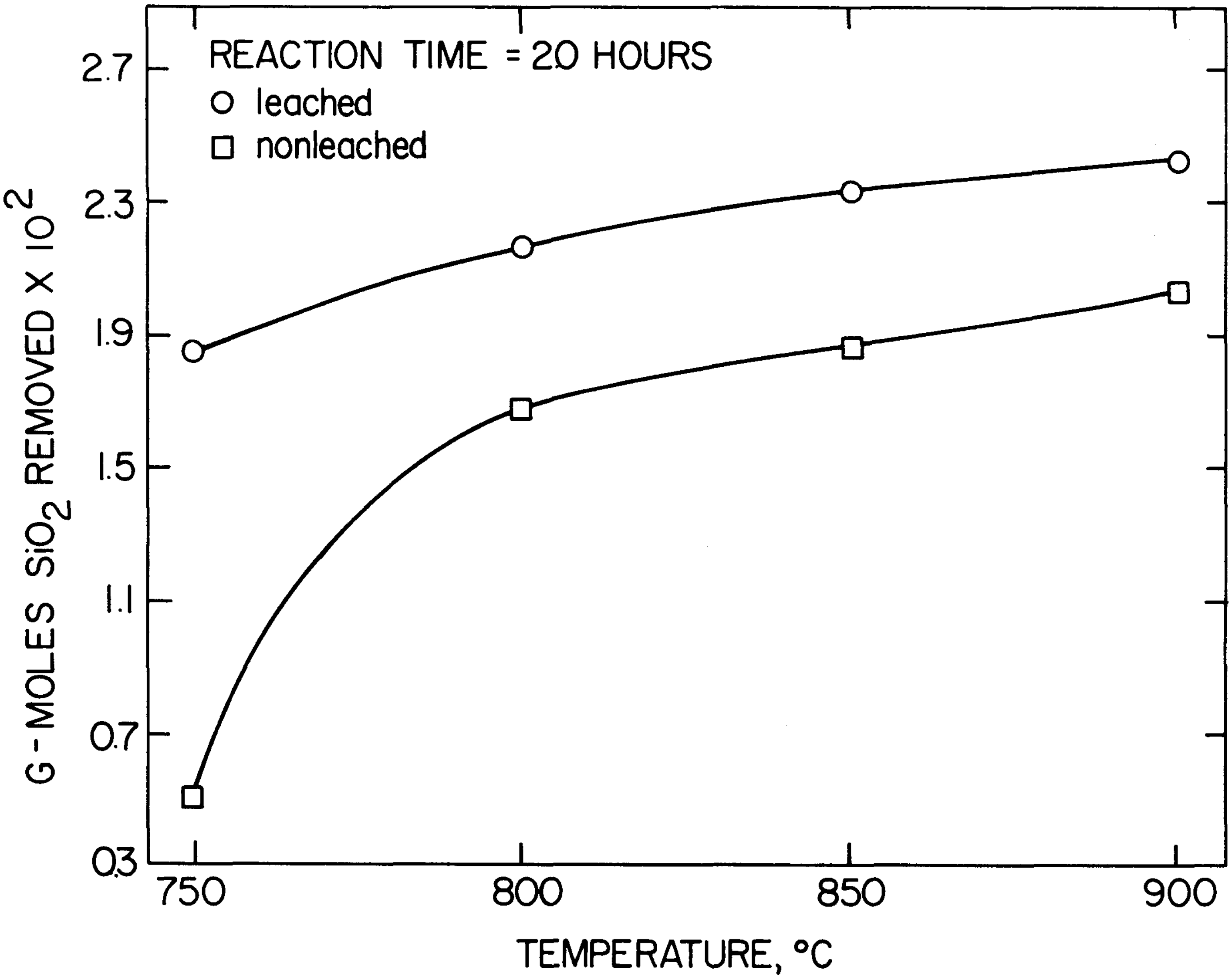

Figure 9. The effect of temperature on the g-moles silica removed for leached and nonleached fly ash samples. Chlorine feed rate = 0.0010 g-moles/min

Table 5. Moles x 10^3 and mole percents of oxides removed for the chlorinations of leached nonmagnetic fly ash samples

			Metal oxide			
Run number	Temp. °C	Time min.	Al_2O_3 moles Mole %	Fe_2O_3 moles Mole %	SiO_2 moles Mole %	TiO_2 moles Mole %
3	750	120	3.152	9.688	29.60	0.697
			85.41	62.28	40.18	74.92
4	800	72	2.750	8.368	23.56	0.606
			74.51	53.77	31.98	65.07
5	850	60	1.524	4.914	14.13	0.320
			82.63	63.19	38.36	68.74
6	800	90	2.936	8.532	26.22	0.601
			79.55	54.85	35.58	64.26
7	800	106	3.102	10.375	30.85	0.691
			84.07	66.70	41.88	73.90
8[a]	800	120	3.040	9.106	27.02	0.642
			82.04	58.56	36.68	68.64
9	850	120	3.153	10.569	30.61	0.688
			85.47	67.96	41.56	73.59
10[a]	850	120	3.245	11.389	32.36	0.731
			87.94	73.21	43.94	78.23
11	750	120	3.110	8.018	23.72	0.650
			84.30	51.56	32.20	69.52
12	750	120	3.179	8.670	26.52	0.691
			86.17	55.75	36.00	73.92
13[a]	750	120	3.239	10.21	30.45	0.715
			86.27	61.45	33.51	76.26
14	800	120	3.137	10.76	21.47	0.663
			83.57	64.79	31.45	70.74
15[a]	900	120	3.465	13.71	31.56	0.798
			92.28	82.53	46.22	85.13
16	900	90	3.293	12.60	28.04	0.750
			87.73	75.83	41.07	79.96

[a] Data from these runs were used in Table 6 and Figures 10-13.

ash is about 2.25 if the 750^{o}C point is ignored, and 2.05 for the leached ash.

The data in Table 4 indicate that the moles alumina removed are comparable for the two-hour nonleached versus leached ash chlorinations. However, there is an appreciable difference between the moles silica removed in these same samples. The data indicate that leached ash had considerably more silica removed. Since the alumina conversions are comparable, it does not appear that the calcium present in the nonleached ash blocked the surface to hinder the reaction. There is evidence that alkali and alkaline earth chlorides enhance alumina and suppress silica reactivities with chlorine (32). However, the effects of calcium were not examined experimentally in this study. It is possible that more silica was removed from leached ash samples because no calcium oxide was chlorinated first. The chlorine was available to the leached ash silica for a greater amount of time. This could also explain why the alumina-silica ratios differ for leached and nonleached ash samples for two-hour chlorinations. The moles of alumina removed reaches a plateau for both leached and nonleached ash somewhere between one and two hours and additional chlorine exposure beyond this point mostly causes more silica to react. This serves to lower the ratio for the leached ash more because more silica is reacted due to a longer exposure time. There is a point between one and two hours where the alumina conversion rate is no longer great enough and the silica rate is too high to justify continuing the reaction.

Several other observations concerning the leached versus nonleached data will be mentioned. In Figure 9, the nonleached ash silica moles removed at 750°C appears to be low. Since the point was not duplicated, no sure judgment can be made as to its authenticity. A plot of the moles of iron oxide removed is not included but comparisons can be made based on the data given in Table 4. About 50-75 percent of the iron oxide was chlorinated within the first hour and 80-90 percent after the second hour. After two hours of chlorination, the amounts of iron oxides removed from either leached or nonleached ash were comparable. The titania ash concentration is low but its chlorination was followed because titanium is quite valuable. Usually there was little difference between the titania conversion for leached and nonleached ash. As a general rule, the titania mole percent conversions for one- and two-hour chlorinations were nearly the same as the alumina conversions. Finally, the number of moles of alumina and silica removed, as shown in Figures 8 and 9, are slightly temperature dependent, suggesting possible kinetic effects.

Acid leaching of fly ash did not significantly influence its chlorination. One advantage to acid leaching is that the calcium oxide concentration is greatly reduced. This simplifies the system and saves chlorine. One possible disadvantage is that nonleached ash appeared to have less silica removed for a given set of reaction conditions. It is important to notice that there was not a clean separation between the three main components, Fe_2O_3, Al_2O_3, and SiO_2, as a result of the preferential chlorination of fly ash. All three components reacted somewhat throughout the chlorination period. Other reaction systems may achieve a separation, but the one used here did not.

Gas Chromatography Chlorinations

Chemical observations

The first set of chlorinations of leached versus nonleached fly ash only considered the changes in the fly ash composition as a function of time and temperature. This is only part of the picture because both chlorine and carbon are also involved. The second set of chlorinations (where gas chromatography was used) was conducted so information about the chlorine and carbon could be collected. This information, coupled with the leached versus nonleached data, gives a more comprehensive picture of what happened during the chlorination.

Only acid leached fly ash was chlorinated in this second set of experiments. The product gas stream was analyzed using the gas chromatograph. The product stream consisted of carbon monoxide and dioxide, chlorine, and silicon tetrachloride, the only materials not condensed at temperatures above 24°C. As was explained in the experimental section, standard curves and total exit gas flow rates were used to calculate flow rates of CO, CO_2, and Cl_2 as a function of reaction time. The silicon tetrachloride exit flow rate was calculated by difference. No standard GC curves were run for $SiCl_4$, but, since the sample loop volume was known to be 2.5 ml and the other three component volumes could be calculated from the chromatograms, the $SiCl_4$ volume in the loop could be determined. The volume percent was calculated and multiplied by the total exit flow rate to get the $SiCl_4$ flow rate. No $SiCl_4$ peak could be obtained on the GC because to separate the other components, the separation column was held at 0°C, a temperature at which $SiCl_4$ condenses. Most of the $SiCl_4$ condensed on the column and the small part that did carry through only raised the GC recorder base line slightly.

Figures 10, 11, 12, and 13 are plots of flows of Cl_2, $SiCl_4$, CO, and CO_2, respectively, for chlorinations done at the four temperatures, 750, 800, 850, and 900°C. Points were taken from the graphs every 2.5 minutes and the values were punched onto computer cards. A computer program was written to integrate the area under the curves to give g-mole totals for 10-minute intervals. A five-point Simpson's approximation integration scheme was used. The program was also used to calculate oxygen output at 10-minute intervals, two-hour g-mole totals for CO, CO_2, O_2, Cl_2, and $SiCl_4$, and $CO:CO_2$ ratios.

Chlorine and silicon tetrachloride balance results are listed in Table 6. The amount of chlorine fed was calculated by multiplying the input flow rate by the reaction time and then converting the volume to g-moles using the ideal gas equation. The oxide losses were known from analyses of the residues remaining after the chlorination. By assuming that iron (III) chloride, aluminum trichloride, silicon tetrachloride, and titanium tetrachloride were formed from Fe_2O_3, Al_2O_3, SiO_2, and TiO_2, respectively, the chlorine used to form chlorides was determined. The integrated chlorine exit flow rate versus reaction time results gave the amount of unreacted chlorine. Finally, the chlorine fed minus both the chlorine used and the excess should balance. The percent discrepancies are listed in Table 6.

Assuming that the chlorides are formed from the oxides listed may seem like a poor idea because as has been mentioned, most of the oxides

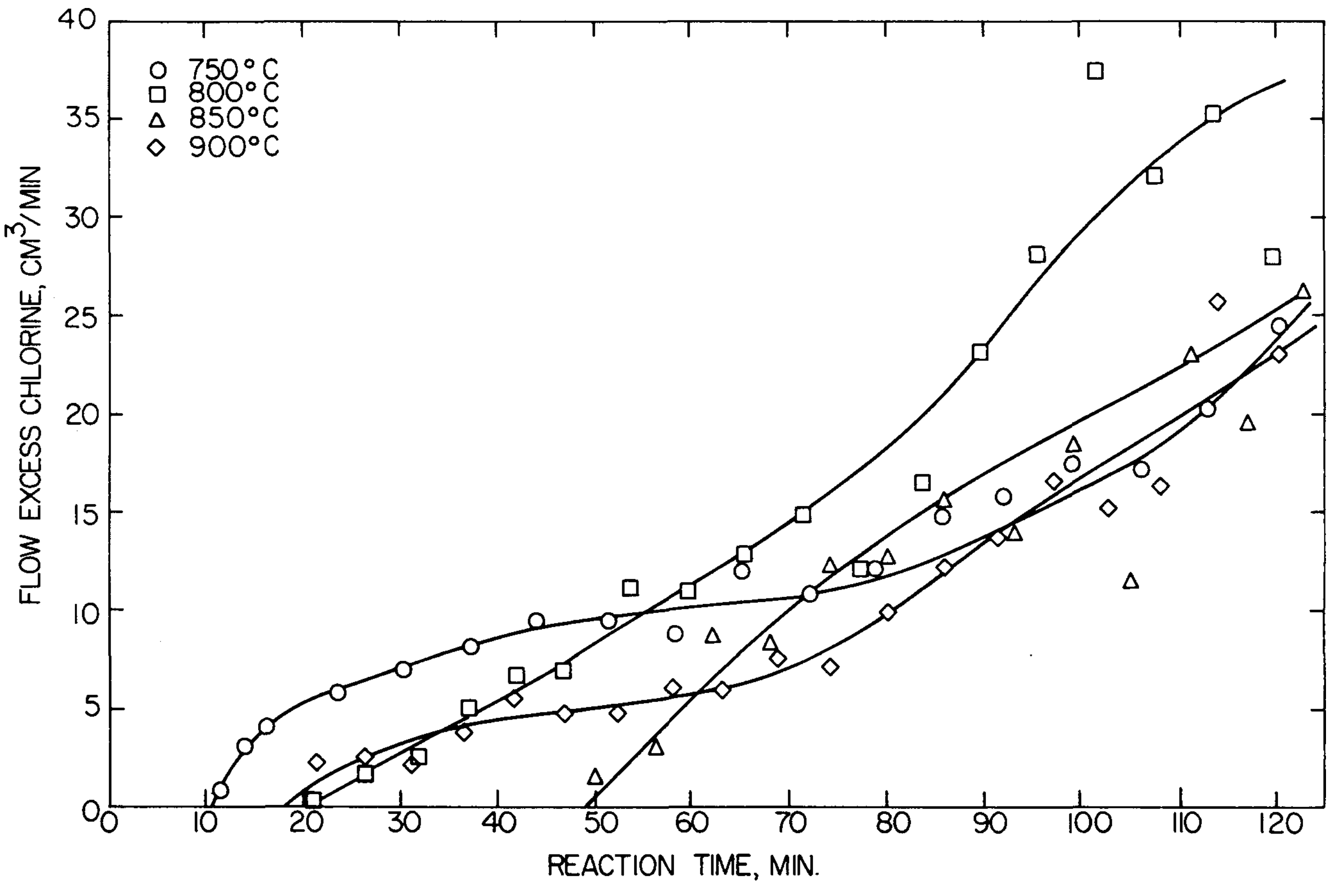

Figure 10. Flow rate of excess chlorine as a function of reaction time at different temperatures. Chlorine feed rate = 0.0013 g-moles/min

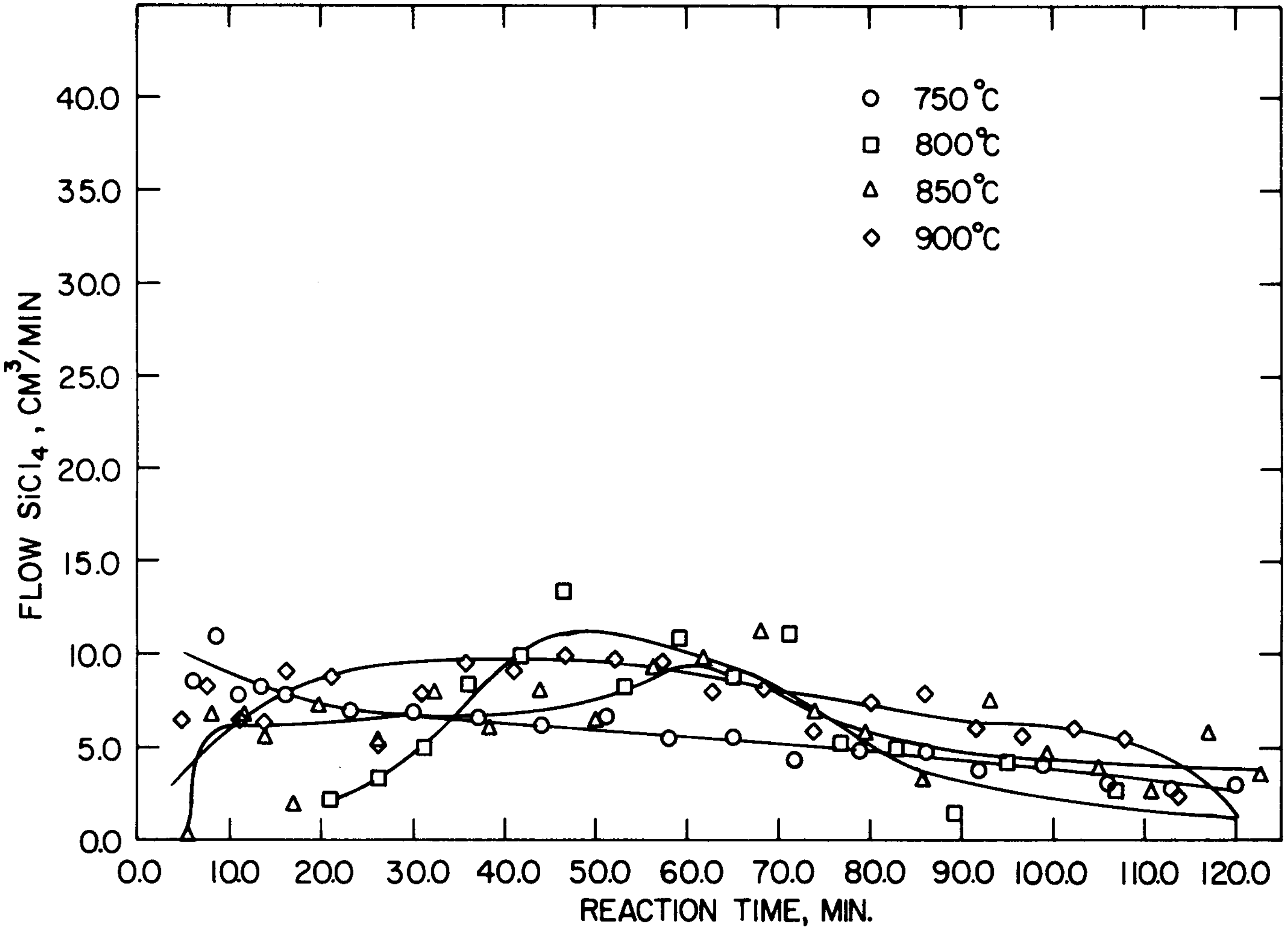

Figure 11. Flow rate of $SiCl_4$ produced as a function of reaction time at different temperatures. Chlorine feed rate = 0.0013 g-moles/min

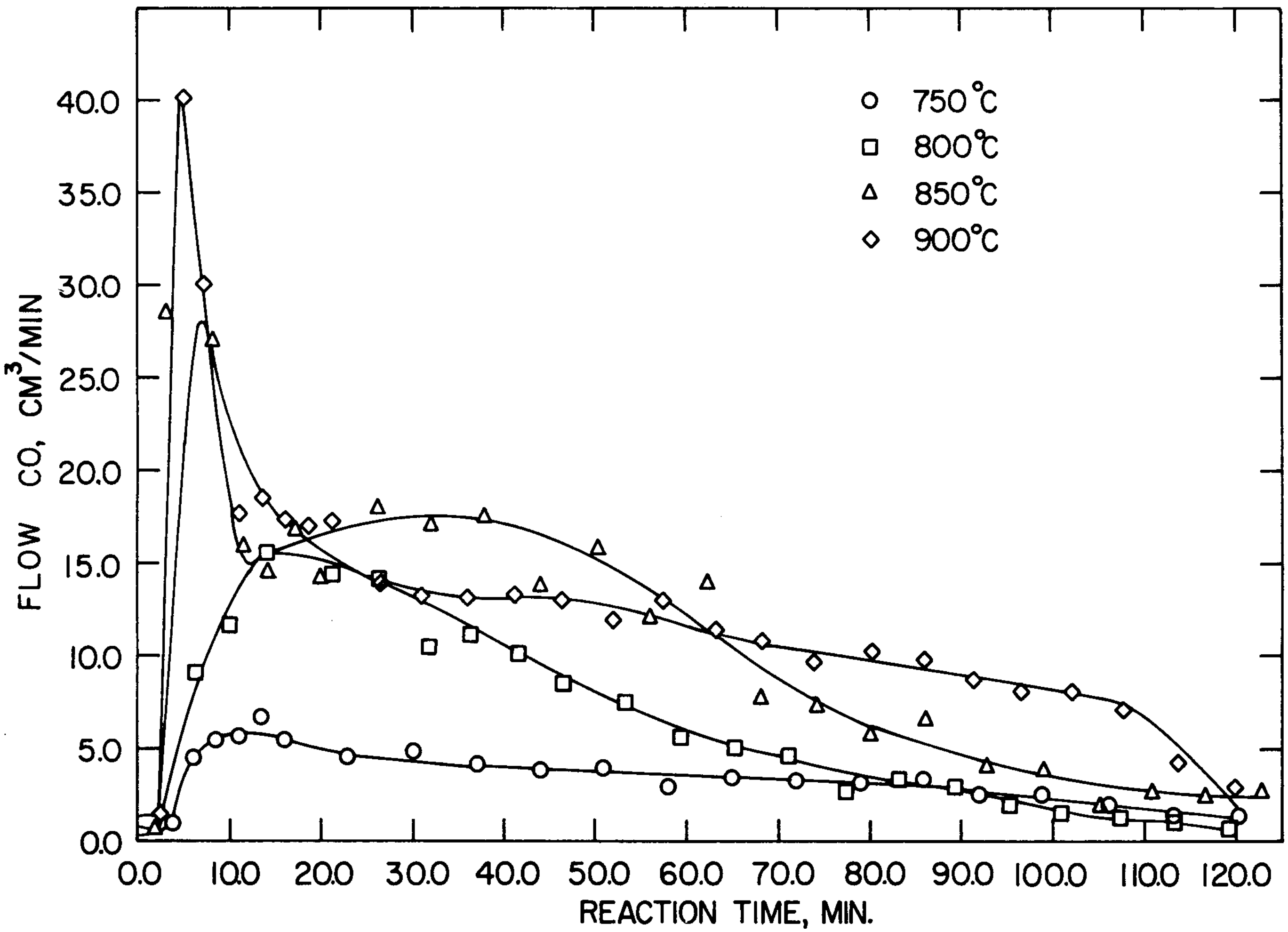

Figure 12. Flow rate of CO produced as a function of reaction time at different temperatures. Chlorine feed rate = 0.0013 g-moles/min

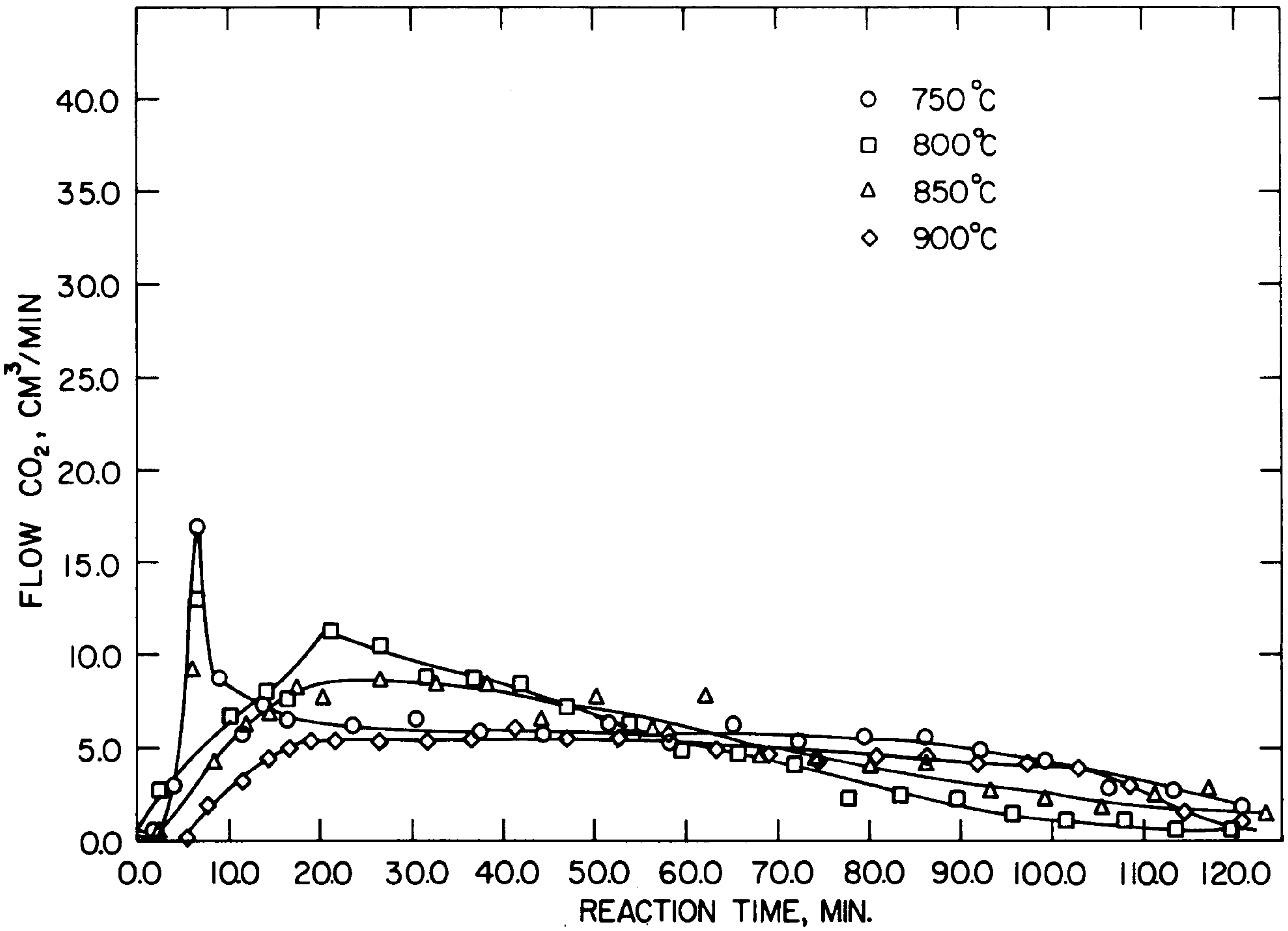

Figure 13. Flow rate of CO_2 produced as a function of reaction time at different temperatures. Chlorine feed rate = 0.0013 g-moles/min

Table 6. Chlorine, silicon tetrachloride, and oxygen balances for four chlorinations of leached, nonmagnetic fly ash samples

Temp. °C	Cl_2 fed g-moles	Cl_2 used g-moles	Cl_2 out g-moles	% dis.[a] Cl_2	SiO_2[b] g-moles	SiO_2[c] g-moles	% dis.[d] SiO_2	Pro. O_2[e] / Act. O_2
750	0.1607	0.1027	0.0506	4.6	0.0304	0.0259	15.0	1.5
800	0.1519	0.0918	0.0668	4.4	0.0270	0.0263	2.6	1.1
850	0.1519	0.1101	0.0411	0.4	0.0324	0.0283	12.6	1.1
900	0.1609	0.1162	0.0424	1.4	0.0316	0.0351	11.3	1.2

[a] The percent discrepancy in the chlorine balance.

[b] The g-moles silica removed from the fly ash samples based on solid residue analyses.

[c] The g-moles silica removed from the fly ash samples based on gas chromatographic analyses.

[d] The percent discrepancy in the silica balance.

[e] The ratio of the amount of oxygen removed based on residue analyses to the amount removed based on gas chromatographic analyses.

in fly ash are not in these forms. However, prior to the analysis of unchlorinated and chlorinated ash samples, they are brought to a common chemical basis by ashing the samples at 900°C overnight in an oxygen atmosphere. It is safe to assume then that most of the metals in both samples are in their most stable oxidized form prior to analysis. Therefore, the component losses used to calculate the amount of chlorine needed to form chlorides are accurate based on the oxides listed.

The silicon tetrachloride balances were a good test of overall data accuracy. Since all GC errors were essentially lumped into the silicon tetrachloride numbers, a large error in these results would most likely indicate that either the residue analyses were not accurate, or else the CO, CO_2, and Cl_2 standard curves were in error. The percent discrepancies for the silicon tetrachloride balances are listed in Table 6.

The excess chlorine flow versus reaction time curves are plotted in Figure 10. The 750 and 800°C runs released comparable amounts of excess chlorine as did the 850 and 900°C runs. The curves in Figure 11 show that fairly constant amounts of silicon tetrachloride are evolved throughout the chlorination. It would be expected that as the iron and aluminum oxide contents were depleted, that the silicon tetrachloride production would increase; however, as Figure 11 shows, its production also decreases with reaction time. Reasons for this behavior will be mentioned later.

The data from Figures 10-13, combined with the leached versus non-leached data, describe what happened to each major component of the reaction system during chlorination. Usually, equipped with such data, one could readily determine reaction mechanisms and limitations and parameters such as activation energies. However, the system used was too specific. The data describe a reaction system where ten grams of a 10:3 C-1 nonmagnetic fly ash to graphite mixture was reacted with a flow of 0.0010 g-moles chlorine per minute in a horizontal fixed-bed reactor. The most troublesome aspect is that the chlorine flow was so small that the conversion of chlorine varied from complete to almost no conversion during the course of a chlorination. The reactant and product gas compositions, therefore, changed radically during a chlorination so that models used to describe such gas-solid reaction systems cannot be applied.

The Boudouard reaction ($CO_2 + C = 2CO$) could affect the data. The metal oxide components can be reduced by either carbon or carbon monoxide. However, because the Boudouard reaction converts carbon and carbon dioxide to carbon monoxide, it is not possible to determine to what extent the two reductants are utilized. Since only one composition of carbon was employed, the data cannot be used to determine what effect the reaction had.

Even though the reaction system cannot be fully parameterized using the data obtained, some useful observations will be made. Figure 12 shows that the flow of carbon monoxide evolved during the reaction varied with temperature and reaction time. The carbon monoxide flow and the height of the initial spike increased with temperature. A paper (23) in which the iron oxides in ilmenite were reduced by carbon monoxide showed a similar spike except that it was for carbon dioxide production. The carbon monoxide spike obtained in Figure 12 is possibly a direct result of the Boudouard reaction.

During the reactor heat-up period and just prior to the introduction of chlorine, small amounts of carbon monoxide and dioxide were detected in the reactor purge stream. This would indicate that carbon is a poor primary reductant. Figure 12 shows that when the chlorine was introduced at zero time, varying amounts of carbon monoxide were evolved. Since the carbon alone was not reducing the oxides at an appreciable rate, the chlorine must initiate some mechanism that frees oxygen to form carbon monoxide and dioxide.

Thermodynamically, it was shown that none of the proposed metal oxides can react directly with chlorine to produce free oxygen for temperatures of 600-1000°C. However, since it is not known exactly which oxides are being chlorinated, it is possible that the oxides that are actually present can be directly chlorinated to give free oxygen. The carbon could also be serving as a site for the formation of chlorine containing free radicals which could react with the metal oxides. This type of mechanism was proposed in two Russian abstracts (25, 47). If the free radical mechanism is prominent, then the amount of carbon oxides formed depends largely on which free radicals are present. A radical such as $C\text{-}Cl_2$ attacking the metal oxide surface would produce carbon monoxide; however, if COCl is transferred to the fly ash surface, carbon dioxide would be formed.

Figure 13 is a plot of the carbon dioxide flow rate versus reaction time. Here the spike trend is the opposite of that in Figure 12. The carbon dioxide spike is the highest at the lowest temperature and does not exist at the highest temperature. As in the case of carbon monoxide in Figure 12, the production of carbon dioxide depends on the reaction mechanism. One does know that the amount of carbon dioxide produced is not increased by the Boudouard reaction. The thermodynamic data indicate that carbon monoxide production is favored above about 700°C. Therefore, almost any carbon dioxide formed results from the reaction of carbon monoxide with the metal oxides. The direct reaction of carbon with oxygen to form carbon dioxide in one step is very unlikely (4).

Using thermodynamic data (14), the CO/CO_2 ratio was calculated as about 3 at 750°C and 30 at 900°C. In making these calculations, it was necessary to assume that the carbon activity was 1 and that the sum of the partial pressures of carbon monoxide and dioxide was about 0.7 atm. The CO/CO_2 ratios obtained experimentally ranged from 0.7 at 750°C to 2.5 at 900°C. The experimental CO/CO_2 ratios may be low because the carbon was not of unit activity. Another possibility is that the system did not reach equilibrium. A Russian paper (48) indicates that at 900°C, about 150 seconds are required for the $CO\text{-}CO_2\text{-}C$ reaction system to reach equilibrium. The maximum residence time in the reactor used here was about 20 seconds. Arthur (4), in an extensive study of the burning of carbon by oxygen, found for short contact times, that the Boudouard reaction had little effect on the product composition.

If the Boudouard reaction does not determine the CO/CO_2 ratio, then the actual chlorination reaction mechanism must. There are many possible contributing factors. The literature review disclosed that carbon is a better reductant at higher temperatures (900°C) and that carbon monoxide is better at lower temperatures (750°C). The data in Figures 12 and 13 support this conclusion in that carbon dioxide is formed in greater quantities at 750°C than is carbon monoxide and that the carbon monoxide production is greater at 900°C. Therefore, as shown in Figure 12, the height of the initial carbon monoxide spikes decrease with temperature because as temperature decreases, less carbon is used as the primary reductant, and so, less carbon monoxide is produced.

Why the data appear as such and why there is a difference between the effectiveness of carbon monoxide and carbon as reductants cannot be answered without knowing the reaction mechanism. Thermodynamics may explain part of the problem. Energetically, carbon monoxide formation is favored over carbon dioxide formation at higher temperatures. The free radical formations can be enhanced by higher temperatures also. At higher temperatures such complexes as $C\text{-}Cl_2$ may be more abundant and at lower temperatures, COCl radicals may be present. It is also possible that as the temperature is raised, more direct substitution of oxygen by chlorine occurs. This would give rise to more carbon monoxide. However, at the present level of understanding of this very complex system, it seems safest to say that at 750°C, carbon monoxide serves as the primary reductant and that at 900°C, carbon serves as the main reductant. In addition, the difference in the effectiveness of carbon and carbon monoxide as reductants seems to arise due to mechanistic and/or kinetic effects.

The oxygen evolution rate during the chlorination is a reasonable measure of reaction rate. The carbon monoxide and dioxide flow rates versus reaction time plots were integrated over 10-minute intervals and the results manipulated so as to give the oxygen totals as a function of reaction time. The results are plotted in Figure 14 for different temperatures. The total amount of oxygen evolved increases with temperature. The amount of oxygen that should have been evolved after two hours of chlorination, based on the fly ash constituents being Fe_2O_3, Al_2O_3, SiO_2, and TiO_2, was calculated by knowing the amounts of each removed during the chlorination. The actual amount of oxygen removed after two hours is known from Figure 14. The ratios of projected oxygen removed to actual are listed in Table 6. The ratios for 800, 850, and 900°C are comparable at 1.1-1.2, however, the 750°C ratio is 1.5. First, the ratios being greater than unity indicate that the projected compounds are not those actually present in the fly ash. Also, the fact that the 750°C ratio is higher than the others could mean that the fly ash reacted at 750°C is in a less reduced state. There may be more oxygen present in unreacted ash held at 750°C than in ash held at 800°C or higher.

Figure 15 is a plot of the carbon conversion versus fly ash conversion. The carbon conversion is calculated by dividing the amount of carbon removed in the form of carbon monoxide and dioxide by the total carbon initially present. The total carbon includes both the added graphite and the unburned carbon already present in the ash. The fly ash conversion is the sum of iron, aluminum, silicon, and titanium oxides removed divided by the total originally present. The different temperatures are indicated by symbols. The 800, 850, and 900°C data points collectively roughly approximate a straight line. This indicates

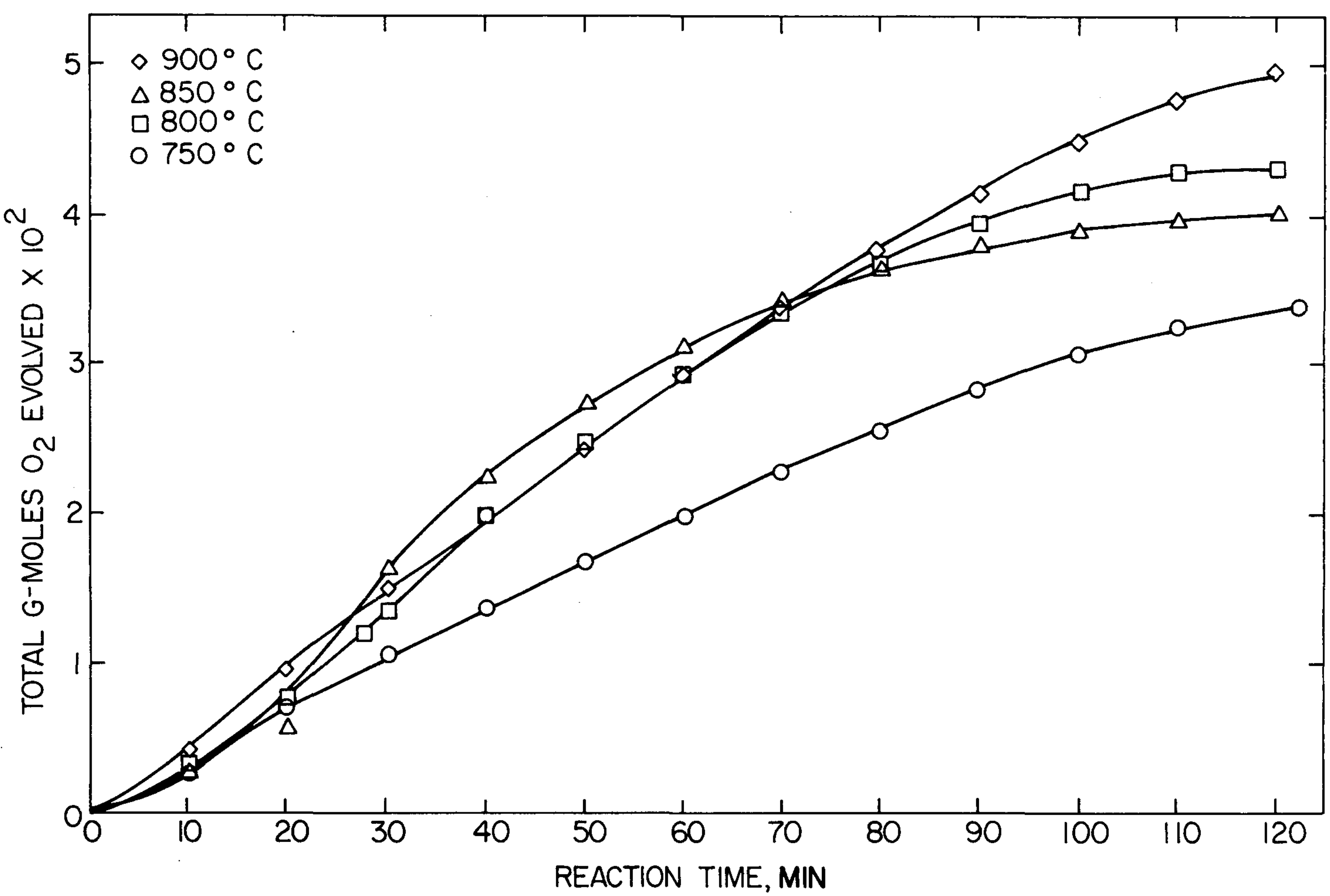

Figure 14. Total g-moles of oxygen produced as a function of reaction time at different temperatures. Chlorine feed rate = 0.0013 g-moles/min

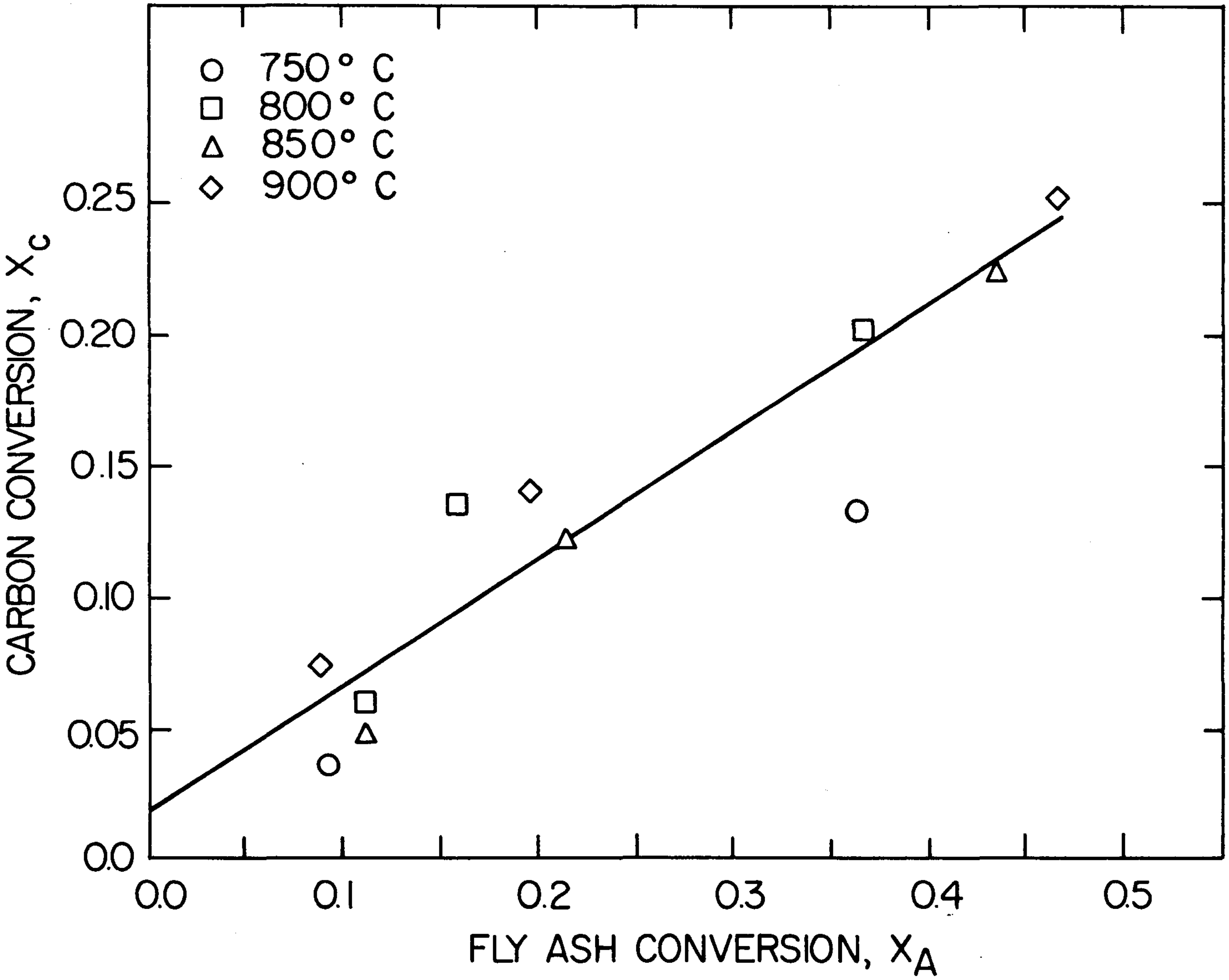

Figure 15. The effect of fly ash conversion on carbon conversion at different temperatures

that for a given carbon conversion, a certain fly ash conversion is obtained regardless of the temperature.

Previously, it was mentioned that the ratio of the projected amount of oxygen removed to the actual amount removed was nearly constant for 800, 850, and 900°C. Since the oxygen can be removed in the form of carbon monoxide or dioxide, then if the constant projected to actual oxygen removal ratio and the straight line relationship between carbon and fly ash conversions hold, the amount of either carbon monoxide or dioxide evolved must be constant for the three temperatures. If Figures 12 and 13 are considered, it is apparent that the carbon dioxide flow is nearly constant for the three highest temperatures. This could indicate that one component, such as iron oxide could be chlorinated based on a certain mechanism involving carbon dioxide or that a constant amount of a certain radical that gives rise to carbon dioxide upon reaction with ash is formed for all three temperatures. The 750°C points in Figure 15 lie below the line indicating that less carbon was used for a given ash conversion. This is directly related back to the results in Figure 14 where it was pointed out that significantly less oxygen was removed and to Figure 15 where it was shown that the carbon conversions were less for a given fly ash conversion.

Physical observations

The actual chemical reaction part of the overall process of chlorinating fly ash may not be important in determining the reaction rates and final conversions. Other physical effects such as mass transfer can be crucial (46). Factors like the carbon proximity and surface area of the primary reactant were shown to control chlorination reaction rates in the literature. Therefore, rather than ignoring the physical factors, as all previous publications (10, 50, 52) concerning fly ash chlorination have, data were collected that physically describe the fly ash at various degrees of conversion.

Two types of mass transfer limitations can occur. Boundary layer mass transfer controls if the reactant and product gases do not travel through the stagnant boundary layer surrounding the particles fast enough to satisfy either the kinetic capabilities or thermodynamic conditions of the reactions on the solid surface. Pore diffusion controls if the reactant and product gases do not enter and leave the pores fast enough to satisfy the same two conditions. Particle size distributions and surface area measurements at different degrees of fly ash conversion will help to determine whether mass transfer limitations are important.

Both particle size distributions and surface area measurements were obtained. A Coulter Counter was used to obtain the particle size distributions shown in Table 7. The diameter listed is an average for a given size range. The particle diameters falling in a particular channel vary over a range of approximately one-half the difference between the diameters of the channels on either side. The original data were normalized so an equal number of particles were counted for each sample. There is not a significant difference in the particle size distributions as a function of conversion. This could be due to the fact that the mole percent conversions were not greatly different.

Table 7. Particle size distribution of leached, nonmagnetic fly ash samples chlorinated for two hours

Avg. dia. microns	Temp, °C 750 # cts.[a]	 800 # cts.	 900 # cts.
40.3	3	0	0
36.2	22	6	4
28.7	106	30	28
22.4	182	77	70
18.1	418	247	236
14.4	669	475	527
11.4	1,092	890	978
9.04	1,590	1,490	1,658
7.18	2,388	2,306	2,471
5.70	3,724	3,583	4,105
4.52	5,403	5,531	5,818
3.58	7,746	8,024	8,251
2.84	10,144	10,361	10,336
2.26	14,060	14,526	13,066

[a] # cts. is the number of counts registered on the Coulter counter with the corresponding average diameters given.

The conversion at 800°C is 29.3 mole percent, 36.3 mole percent at 750°C, and 46.2 mole percent at 900°C. However, it is more likely that the particles are hollowed out so that they approximate the same size for a wide conversion range.

Surface area measurements were collected using a Micromeritics BET instrument. The areas are plotted as a function of fly ash conversion in Figure 16. No distinction was made between points collected for ash chlorinated at different temperatures. The fly ash conversion is the sum of the moles of Fe_2O_3, Al_2O_3, SiO_2, and TiO_2 removed divided by the total originally present. The data are not conclusive, but it appears that the surface area increases with conversion initially, peaks at about 20 percent fly ash conversion, and then decreases with conversion. The increase could be caused by particles developing pores due to reaction and the decrease caused by the pores growing together as the reaction proceeds. This conclusion is consistent with the hollowing out idea mentioned for the particle size distributions. Should the pores grow together, there would still be projections present on the individual particles that would cause them to be counted as particles of the original size by the Coulter counter.

The data in Table 7 indicate that the fly ash-carbon mixture average particle diameter is about 5 microns for material chlorinated for only one-half hour at 900°C. Pore diffusion limitations would be very unlikely for a system using such small particles because the diffusion path lengths are very short. Mass transfer limitations in the form of diffusion of products or reactants through a stagnant gas boundary layer surrounding each particle is possible. This was not tested for

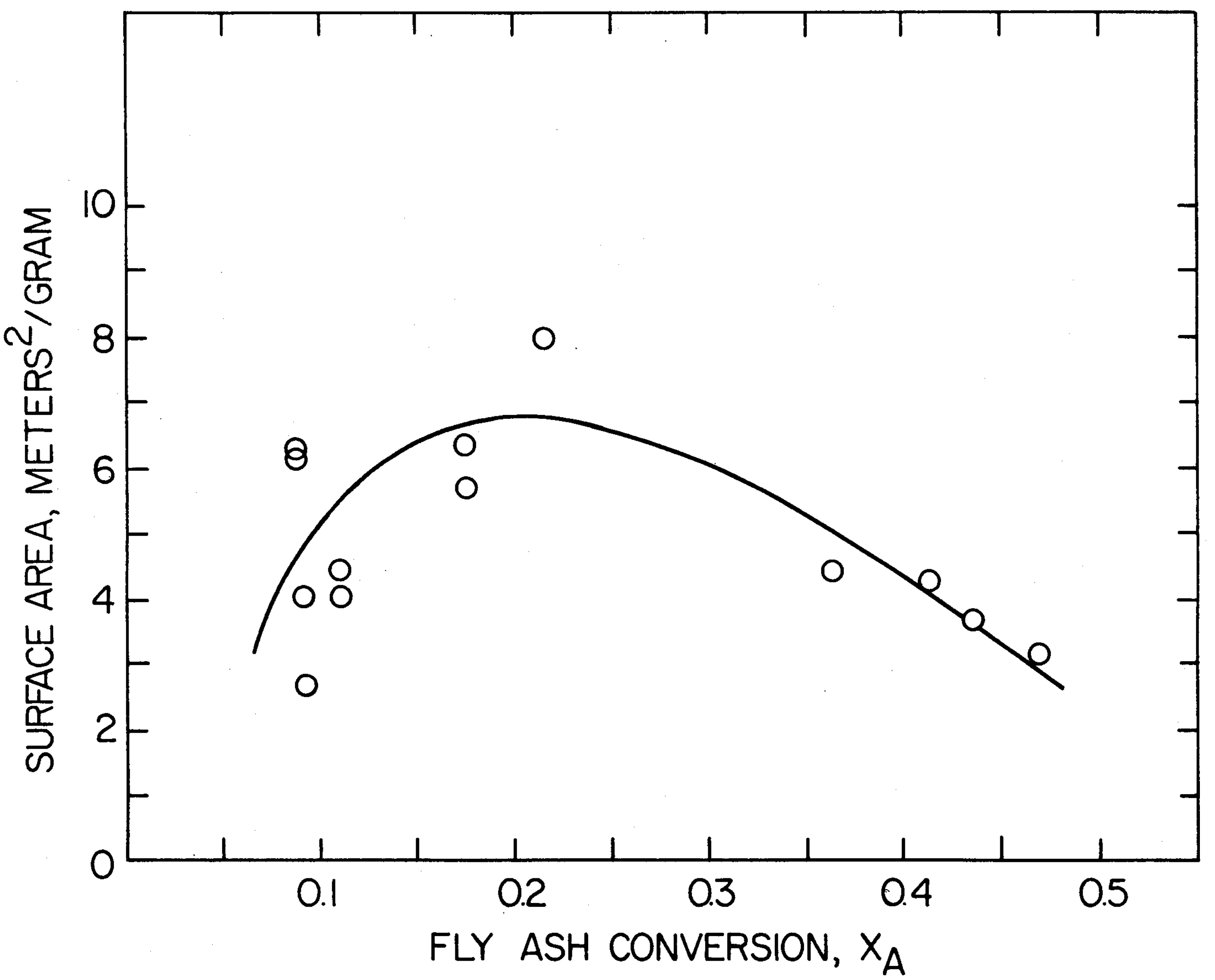

Figure 16. The effect of fly ash conversion on sample surface area

directly because only one feed velocity was used and the total exit gas flow rate measured with the bubble flow meter did not vary significantly during the runs. However, since the particles stayed nearly the same diameter as a function of conversion, the stagnant gas layer thickness should not have changed during the reaction. If mass transfer through the stagnant layer controlled the reaction, the diffusion rate through the boundary layer would have had to decrease with conversion to account for the drastic drop in reaction rate as a function of conversion observed. This would be possible only if a solid product layer was formed as a result of reaction. However, no layer was observed when chlorinated ash was viewed with a scanning electron microscope (SEM) and also, the products are predicted to be volatile chlorides. Therefore, boundary-layer mass transfer cannot be used to explain the extreme drop in reaction rate of silica at 110 minutes observed in Figure 11.

Scanning Electron Microscope Results

One other method was employed to gain some information about fly ash constituent distributions as a function of conversion. Four leached ash samples were mounted on plastic discs, polished to give cross sections, and examined with a scanning electron microscope. The first sample was not chlorinated, and the other three were chlorinated at 900°C for one-half, one, and two hours, respectively. The SEM used has a microprobe attachment which allowed for X-ray fluorescence analysis of the ash surfaces. The objective of this study was to determine if individual ash particles are homogeneous in composition as a function of diameter before and/or after chlorination.

Many individual particles need to be analyzed to make such a study statistically accurate. Only about 10 particles were analyzed per sample so the results are possibly not representative of the sample; however, some very prominent results will be mentioned. All particles were of homogeneous composition across their cross-sectional surface except where an area appeared to have a contrasting color when viewed by the SEM. The composition could then be radically different. These areas appeared to be small inclusions of material containing high concentrations of iron.

There was often large composition differences between particles in the same sample. If iron was present in nonchlorinated ash particles, its composition was always nearly 30 weight percent. However, sometimes the particles contained only aluminum and silicon and no iron. As the fly ash conversion increased, the silicon to aluminum weight percent ratio increased. Also, for all three chlorinated samples, the iron content stayed at a fairly constant level. This constant level of iron in reacted ash could be a result of either iron being trapped within the particles in an inaccessible location or certain iron containing compounds not being reactive.

One final observation deals with differences in composition of the particles as a function of their geometry. Typically, fly ash is composed of spherical particles. This was observed on the SEM for the analyses of nonchlorinated ash. Fly ash that had been chlorinated contained greater numbers of irregularly shaped particles than did nonchlorinated ash. In almost all cases, the fragments were composed of only silicon. Occasionally, very small amounts of aluminum and iron were present. The fragmentation could have occurred during the mixing of the fly ash with graphite in a ball mill prior to chlorination. The nonchlorinated, nonfragmented ash sample was not mixed with graphite in a ball mill. The fragmentation could also be caused by thermal shock. The ash is heated to high temperatures rapidly prior to chlorination. The silicon fragments seen in the chlorinated ash could be pieces of spheres that had the aluminum and iron removed from them by chlorination. The iron and aluminum could be removed more readily because the fragments had more exposed surfaces. This removal of aluminum from the fragments has important implications for the overall process.

CONCLUSIONS

General Observations

Throughout the thermodynamic, experimental, and results and discussion sections, ideas and observations have been mentioned concerning a wide variety of subjects related to the chlorination reactions. These observations will be listed and followed by a discussion of conclusions concerning the probable chlorination reaction limitations. All observations listed apply to chlorination reactions conducted at a pressure of 1 atmosphere and over a temperature range of 750-900°C.

1. Thermodynamically, the direct reaction of chlorine with Fe_2O_3, Al_2O_3, SiO_2, or TiO_2 is not favored.
2. The reactions of chlorine and carbon with Fe_2O_3, Al_2O_3, SiO_2, and TiO_2 have large negative Gibb's free energy changes and are mostly exothermic.
3. The Gibb's free energy changes favor the reaction of silicon tetrachloride with Al_2O_3 to form SiO_2 and $AlCl_3$.
4. The acid leaching experiments indicate that 90 weight percent of the calcium oxide present in nonmagnetic fly ash is removed by leaching with 1 molar HCl at 22°C and that the amounts of other elements removed are inappreciable.
5. Atomic absorption spectrophotometry is an excellent method for the analyses of aluminum, silicon, iron, and titanium in the fly ash samples.
6. Calcium compounds in nonmagnetic fly ash react preferentially with the chlorine.

7. Iron, aluminum, titanium, and silicon oxides react with chlorine throughout the two-hour chlorination period. None of these components is totally reacted prior to the initiation of the chlorination of another.
8. The chlorination reaction nearly stops after a two-hour period. The maximum alumina recovery is about 80 weight percent.
9. The silicon oxide reaction rate is nearly constant throughout the reaction period. The rate does not increase as the other component concentrations decrease and drops rapidly after a 110-minute reaction period.
10. The only advantages of acid leaching fly ash prior to chlorination are that the reaction system is simplified and chlorine is conserved due to the removal of calcium compounds.
11. The chlorination of ash is somewhat temperature dependent.
12. The Boudouard reaction does not appear to play an important part in determining the CO/CO_2 ratio because of the short residence times in the reactor.
13. Graphite admixed with ash does not serve as an effective reductant alone.
14. Carbon monoxide is the primary reductant at 750°C but carbon is the primary reductant at 900°C.
15. The flow of CO_2 exiting the reactor is nearly constant with temperature but the CO flow increases with temperature.
16. The graphite conversion is directly proportional to the ash conversion for temperatures of 800°C to 900°C.

17. Particle size distributions of ash do not appear to be a function of ash conversions in the range of 0.29 and 0.46.
18. The specific surface area of nonmagnetic fly ash increases with ash conversion up to 0.20 conversion and then decreases with conversion.
19. The composition of chlorinated and nonchlorinated nonmagnetic fly ash particles as a function of diameter is constant except for particles containing inclusions.
20. Partially chlorinated nonmagnetic ash contains fragmented particles composed only of silica.

Reaction Limitations

Chemical control can be due to thermodynamic and/or kinetic limitations. The thermodynamic section indicated that the Gibb's free energy changes are large and negative for the oxides chlorinated in the presence of carbon. Since neither the chlorinations nor the reductions will occur without both chlorine and carbon being present, it appears that some form of gaseous intermediates play a key role in the reactions.

When gaseous intermediates are involved, kinetics become important. The reactions were shown to be nearly all exothermic. Therefore, if there were thermodynamic limitations, an increase in reaction temperature should have hindered the reaction rate. Instead, the reaction rate increased with an increase in the temperature. This would indicate that the improvement in kinetics due to an increase in temperature outweighed any detrimental effects introduced into the thermodynamics. Thermodynamic control is also very doubtful because of the reactor system used. In such a flow system, products are continuously swept away so the equilibria for the reactions would be far to the right. Therefore, kinetic control is a possible reaction rate limitation but thermodynamics is not.

It has been mentioned that mass transfer limitations in the form of diffusion through the gas layer surrounding ash particles or diffusion in and out of pores is doubtful due to the disproportionate change in reaction rate as a function of conversion and to the short diffusion paths in fly ash particles. No relation between surface area and reaction rate in the form of oxygen evolution rate could be found that would indicate surface area limitations. Also, during the first one-half hour of the chlorinations, the surface areas increased but the reaction rate did not. A mass transfer problem could arise if chlorine channelled through the bed instead of dispersing. With such small particles, the chlorine may not have been distributed evenly throughout the bed.

None of the above arguments concerning limitations can explain why the chlorination reaction essentially stopped after about 110 minutes for all four temperatures tested. In the literature review, it was mentioned that several authors found the distance between carbon and the material being chlorinated important. Materials that had a carbon coating throughout their pore system reacted much more rapidly and to a much greater extent than did materials that had been merely mixed with carbon. Limited final conversions similar to those obtained in this study were often explained in terms of a loss of carbon contact. This is the only reasonable suggestion to date to explain the termination of reaction at 110 minutes for the experiments done here. It appears as though kinetics and/or boundary layer mass transfer controlled the chlorination for low ash conversions but that the conversion was ultimately limited due to the loss of ash-carbon contact.

RECOMMENDATIONS

An approach as outlined by Szekely, et al. (46) should be followed in designing experiments used in the further study of the chlorination of fly ash. The main points from that approach along with other ideas are listed below.

1. Chlorinate fly ash that is more representative of ashes being produced today. The fly ash used in this study was a bituminous ash that was collected mechanically. Most ash is now collected both by mechanical and electrostatic precipitators. The electrostatic precipitators collect the smaller particles, which, when mixed with the mechanically separated portion, serves to lower the average particle diameter of an ash sample. Also, a western lignite ash should be used as opposed to the midwestern bituminous ash studied here. Western ashes are becoming much more abundant and are attractive due to the low level of iron oxides present.
2. Use CO-Cl_2 or $COCl_2$ as the secondary reactant combinations. In the literature review, chlorination of admixtures of the primary reactant with carbon were shown to be the slowest and most inefficient.
3. Use an excess of secondary reactants. If a CO-Cl_2 system is used, make sure neither the CO nor Cl_2 conversion is above about 3 percent.
4. Use a down-flow reactor containing a thin bed of fly ash (< 1 cm) for chlorinations. Make the reactor diameter such

that sufficient sample can be used to allow for surface area and pore distribution measurements and for analysis of component losses.

5. Analyze reactor exit gases for CO_2 with a gas chromatograph. Design the GC sampling loop to allow for rapid collection of several gas samples.
6. Position one thermocouple at the center of the reactor near the fly ash bed and another on the outer surface of the reactor for temperature control.
7. Vary the gaseous reactant velocities through the reactor to test for mass transfer effects.
8. Chlorinate samples under conditions where mass transfer does not control the reaction rate and determine activation energies as a function of ash conversion.
9. Investigate the use of sodium chloride as a catalyst.
10. Examine the possibility of increasing the fly ash surface area using thermal shock treatment to fracture the particles.
11. Review the data presently available (10, 52) and decide if silicon tetrachloride recycle through the reactor should be employed as a method for suppressing the chlorination of silica.

BIBLIOGRAPHY

1. Alder, H. P. 1977. Kinetic study of the alumina chlorination with carbon monoxide and chlorine. Light Metals 1: 219-232.

2. Alder, H. P. 1979. The chlorination of alumina. Light Metals 3: 337-350.

3. Analytical methods for atomic absorption spectrophotometry. Revised 1976. Perkin-Elmer Company, Norwalk, Connecticut.

4. Arthur, H. R. 1951. Reactions between carbon and oxygen. Trans. Faraday Soc. 47: 164-178.

5a. Ash importance to increase in coming months. 1977. Ash at Work IX(6). National Ash Association, Washington, D.C.

5b. Barin, I., and O. Knacke. 1973. Thermochemical properties of inorganic substances. Springer-Verlag, New York.

6. Bergholm, A. 1961. Chlorination of rutile. Trans. Metallurg. Soc. AIME 221: 1121-1129.

7. Boar, P. L., and L. K. Ingram. 1970. Comprehensive analysis of coal ash and silicate rocks by atomic-absorption spectrophotometry by a fushion technique. Analyst 95 (Feb.): 124-130.

8. Bruns, J. 1980. A study of midwestern bituminous coal fly ash. M.S. thesis. Iowa State University, Ames, Iowa.

9. Burnet, G., and M. J. Murtha. 1979. Direct utilization — Recovery of minerals from fly ash. Fossil Energy Program Technical Progress Report IS-4655.

10. Chen, C. S. 1979. Chlorination of aluminous materials to produce aluminum chloride. M.S. thesis. South Dakota School of Mines & Technology, Rapid City, South Dakota.

11. Chughtai, A. R., H. M. Harris, and J. R. Riter. 1977. High-temperature heterogeneous equilibria in the unit activity approximation: III. The chlorination of idealized ilmenite in the presence of excess carbon. Metallurg. Trans. B, 8B (Sept.): 507-509.

12. di Corcia, A., P. Ciccioli, and F. Bruner. 1971. Gas chromatography of some reactive gases on graphitized carbon black. J. Chromatogr. 62: 128-131.

13. Dunn, W. E., Jr. 1960. High-temperature chlorination of TiO_2 bearing minerals. Trans. Metallurg. Soc. AIME 218 (Feb.): 6-12.

14. Ellingham, H. J. T. 1944. Reducibility of oxides and sulfides in metallurgical processes. J. Soc. Chem. Ind. (London) 63 (May): 125-133.

15. Fruehan, R. J. 1972. The rate of chlorination of metals and oxides: Part 1. Fe, Ni, and Sn in chlorine. Metallurg. Trans. 3 (Oct.): 2585-2592.

16. Fruehan, R. J., and L. J. Martonik. 1973. The rate of chlorination of metals and oxides: Part II. Iron and nickel in HCl(g). Metallurg. Trans. 4 (Dec.): 2789-2792.

17. Fruehan, R. J., and L. J. Martonik. 1973. The rate of chlorination of metals and oxides: Part III. The rate of chlorination of Fe_2O_3 and NiO in Cl_2 and HCl. Metallurg. Trans. 4 (Dec.): 2793-2797.

18. Harris, H. M., A. W. Henderson, and T. T. Campbell. 1976. Fluidized coke-bed chlorination of ilmenites. U.S. Bureau of Mines Report of Investigations 8165: 1-19.

19. Holliday, R. D., and D. J. Milne. 1975. Experimental evaluation of routes for purification of bauxite by gas-solid reactions. Ind. Eng. Chem., Process Des. Dev. 14 (4): 447-452.

20. Hussein, M. K., A. E. Saba, and K. A. El-Barawy. 1974. Study on the chlorination and beneficiation of Egyptian clays. Egypt. J. Chem. 17 (6): 889-898.

21. Ivashentsev, Ya. I., and V. P. Akimov. 1971. Chemistry of chlorination of metal oxides and the role of the reducing agent in the processes. Sb. Tr. Vses. Mezhvuz. Nauch. Konf. Teor. Protsess. Tsvet. Met. 170 pp.; Chem. Abstr. 77: 79938h (1972).

22. Ivashentsev, Ya. I., and L. N. Pogonina. 1975. Mechanism of TiO_2 chlorination. Zh. Prikl. Khim. 48 (8): 1837-1838; Chem. Abstr. 184176u (1975).

23. Jones, D. G. 1973. Reaction sequences in the reduction of ilmenite: 2-gaseous reduction by carbon monoxide. Proc. Inst. Min. Metall., Trans. C82 (Dec.): 186-192.

24. Kellog, H. H. 1950. Thermodynamic relationships in chlorine metallurgy. Trans. AIME: J. Metals 188 (June): 862-872.

25. Ketov, A. N., M. S. Gaisinovich, E. V. Burmistrova, and A. A. Shligerskii. 1974. Mechanism of chlorination of metal oxides in the solid state. Nauchn. Tr. Gos. Nauchno-Issled. Proektn. Inst. Redkomet. Prom-sti. 16: 13-22; Chem. Abstr. 83: 103907u (1975).

26. Kharkar, D. P., and C. C. Patel. 1952. Chlorination of ilmenite. Curr. Sci. 21 (4): 98-99.

27. Kolthoff, I. M., E. B. Sandell, E. J. Meehan, and S. Bruckenstein. 1969. Quantitative chemical analysis. 4th edition. The Macmillan Company, Toronto, Ontario.

28. Kughetsov, Yu. P., and E. S. Petrov. 1974. Physiochemical study of chlorination of oxide forms of silicon, germanium, and tin. Nauchn. Tr., Gos. Nauchno-Issled. Proektn. Inst. Redkomet. Prom-sti. 58: 23-27; Chem. Abstr. 83: 121335k (1975).

29. Kuruvilla, J., and V. V. Dadape. 1965. Studies in the chlorination of Indian bauxite ores. Indian J. Technol. 3 (81): 244-248.

30. Kuznetsov, Yu. P., E. S. Petrov, and A. I. Vakhrusheva. 1972. Reaction of Si, SiO, and SiO_2 with Cl_2. Izv. Sib. Otd. Akad. Nauk USSR Ser. Khim. Nauk 3: 42-46; Chem. Abstr. 77: 156875q (1972).

31. Landsberg, A. 1975. Chlorination kinetics of aluminum bearing minerals. Metallurg. Trans. B, 6B (June): 207-214.

32. Landsberg, A. 1977. Some factors affecting the chlorination of kaolinic clay. Metallurg. Trans. B, 8B (Sept.): 435-441.

33. Mehrothra, A. K., P. R. Bishnoi, and W. Y. Svrcek. 1979. Metal recovery from coal ash via chlorination — A thermodynamic study. Can. J. Chem. Eng. 57 (April): 225-232.

34. Milne, D. J. 1975. Chlorination of bauxite in the presence of silicon tetrachloride. Metallurg. Trans. B, 6B (Sept.): 486-488.

35. Milne, D. J., and R. D. Holliday. 1975. Thermodynamics of gas-solid reactions for purification of bauxite at moderate temperatures. Ind. Eng. Chem., Process Des. Dev. 14 (4): 442-446.

36. Milne, D. J., and L. J. Wibberley. 1978. Chlorination of alumina and bauxite using pyrolytic carbon as reductant. Light Metals 2: 147-162.

37. Morris, A. J., and R. F. Jensen. 1976. Fluidized-bed chlorination rates of Australian rutile. Metallurg. Trans. B, 7B (March): 89-93.

38. Okahara, Y., and I. Iwasaki. 1970. Chlorination of manganiferous iron ores. Trans. Soc. Min. Eng., AIME 247 (March): 73-80.

39. Patel, C. C., and G. V. Gere. 1960. Some thermodynamical considerations in the chlorination of ilmenite. Trans. Metallurg. Soc. AIME 218 (April): 219-225.

40. Piskunov, I. N., A. K. Orlov, and N. M. Telykov. 1976. Kinetics of the chlorination of nickel oxide and ferric oxide by gaseous hydrogen chloride. Izv. Vyssh. Uchebn. Zaved., Tsvetn. Metall. 19 (4): 15-20. Soviet Nonferrous Metals Research 4 (4): 139-141.

41. Pribil, R., and V. Vesely. 1962. Contribution to the basic problems of complexometry — IX. The determination and masking of alumina. Talanta 9: 23-26.

42. Rowe, L. W., and W. R. Opie. 1955. Production and purification of $TiCl_4$. Trans. AIME, J. Metals 7 (Nov.): 1189-1193.

43. Shelton, R. A. J. 1976. Chloride process metallurgy. International Metals Reviews 21 (Sept.): 141-147.

44. Standard method of analysis of coal and coke ash. 1974. Annual Book of ASTM Standards. ASTM Standard Methods, Philadelphia, Penn. 339 pp.

45. Suhr, N. H., and C. O. Ingamells. 1966. Solution technique for analysis of silicates. Anal. Chem. 38 (6): 730-734.

46. Szekely, J., J. W. Evans, and H. Y. Sohn. 1976. Gas-solid reactions. Academic Press, Inc., New York.

47. Vaks, S. A., G. V. Seryakov, E. P. Strashun, and V. V. Zheltova. 1975. Nauchn. Tr., Gas. Hauchno-Issled. Proektn. Inst. Redkomet. Prom-sti. 58: 3-12; Chem. Abstr. 83: 121334j (1975).

48. Vaskevich, A. D., V. N. Kashtanov, and E. N. Ryzhov. 1975. Mathematical simulation of the gasification of carbon. Izv. Vyssh. Uchebn. Zaved., Tsvetn. Metall. 18 (4): 126-129. Soviet Nonferrous Metals Research 3 (4): 161-162.

49. Vijay, P. L., C. Subramanian, and Ch. Sridhar Rao. 1976. Chlorination of rutile in fluidized beds. Trans. Indian Inst. Metals 29 (5): 355-359.

50. Vogel, A. I. 1961. A textbook of quantitative inorganic analysis including elementary instrumental analysis. 3rd edition. John Wiley and Sons, Inc., New York.

51. Wijatno, H. 1977. Aluminum recovery from coal fly ash by high temperature chlorination. M.S. thesis. Iowa State University, Ames, Iowa.

52. Yuan, P. C. 1979. Chlorination of fly ash and bentonite with a gas mixture of silicon tetrachloride and chlorine. M.S. thesis. South Dakota School of Mines & Technology, Rapid City, South Dakota.

ACKNOWLEDGMENTS

The author would like to thank Dr. George Burnet for his helpful suggestions and guidance throughout this study.

Gratitude is also due to Mike Murtha for his helpful suggestions concerning the experimental system. Finally, sincere appreciation is due to Sylvia Hewitt Stevenson for her encouragement and patience.